2013

Extending the age limit of luminescence dating using the dose-dependent sensitivity of MET-pIRIR signals from K-feldspar

Bo Li
University of Wollongong, bli@uow.edu.au

Zenobia Jacobs
University of Wollongong, zenobia@uow.edu.au

Richard G. Roberts
University of Wollongong, rgrob@uow.edu.au

Sheng-Hua Li
University of Hong Kong

Publication Details

Li, B., Jacobs, Z., Roberts, R. G. & Li, S. (2013). Extending the age limit of luminescence dating using the dose-dependent sensitivity of MET-pIRIR signals from K-feldspar. Quaternary Geochronology, 17 55-67.

Extending the age limit of luminescence dating using the dose-dependent sensitivity of MET-pIRIR signals from K-feldspar

Abstract
We investigated the sensitivity change of multiple-elevated-temperature (MET) stimulated post-infrared infrared-stimulated luminescence (MET-pIRIR) signals as a response to irradiation, sunlight bleaching and heating using samples from the Mu Us Desert, central China. A strong dose dependence of MET-pIRIR signal sensitivity was observed. The intensity of the test-dose signals (Tx) increase with the pre-dose received. Furthermore, the signal sensitivity can be reset by sunlight bleaching or heating. This suggests that both the electron traps and hole centres in K-feldspar can be bleached by sunlight, and can, therefore, be used for dating. Using the test-dose signal as a monitor for sensitivity change, it was found that the sensitivity (or hole centres) saturate at a higher dose (D0 = ~750 Gy) than the sensitivity-corrected signals (or electron traps) (D0 = ~400 Gy). We propose a multi-aliquot regenerative-dose (MAR) MET-pIRIR dating protocol, which utilises the high saturation dose of hole centres. This protocol was tested using aeolian sediments from north China with ages ranging from 0 to 470 ka. It was found that, compared to the dose limit of ~800–1000 Gy using the normal MET-pIRIR or pIRIR procedure, the new method can measure a natural dose of up to ~1500 Gy and produce ages consistent with the expected ages for the samples investigated.

Keywords
k, feldspar, signals, extending, pirir, age, met, limit, luminescence, dating, dose, dependent, sensitivity, CAS

Disciplines
Medicine and Health Sciences | Social and Behavioral Sciences

Publication Details
Li, B., Jacobs, Z., Roberts, R. G. & Li, S. (2013). Extending the age limit of luminescence dating using the dose-dependent sensitivity of MET-pIRIR signals from K-feldspar. Quaternary Geochronology, 17 55-67.

Extending the age limit of luminescence dating using the dose-dependent sensitivity of MET-pIRIR signals from K-feldspar

Bo Li[1,*], Zenobia Jacobs[1], Richard G. Roberts[1], Sheng-Hua Li [2]

[1] Centre for Archaeological Science, School of Earth and Environmental Sciences, University of Wollongong, Wollongong, NSW 2522, Australia

[2] Department of Earth Sciences, The University of Hong Kong, Pokfulam Road, Hong Kong, China

*Corresponding author: bli@uow.edu.au

Abstract

We investigated the sensitivity change of multiple-elevated-temperature (MET) stimulated post-infrared infrared-stimulated luminescence (MET-pIRIR) signals as a response to irradiation, sunlight bleaching and heating using samples from the Mu Us Desert, central China. A strong dose dependence of MET-pIRIR signal sensitivity was observed. The intensity of the test-dose signals (T_x) increase with the pre-dose received. Furthermore, the signal sensitivity can be reset by sunlight bleaching or heating. This suggests that both the electron traps and hole centres in K-feldspar can be bleached by sunlight, and can, therefore, be used for dating. Using the test-dose signal as a monitor for sensitivity change, it was found that the sensitivity (or hole centres) saturate at a higher dose (D_0 = ~750 Gy) than the sensitivity-corrected signals (or electron traps) (D_0 = ~400 Gy). We propose a multi-aliquot regenerative-dose (MAR) MET-pIRIR dating protocol, which utilises the high saturation dose of hole centres. This protocol was tested using aeolian sediments from north China with ages ranging from 0 to 470 ka. It was found that, compared to the dose limit of ~800-1000 Gy using the normal MET-pIRIR or pIRIR procedure, the new method can measure a natural dose of up to ~1500 Gy and produce ages consistent with the expected ages for the samples investigated.

Keywords: K-feldspar, infrared stimulated luminescence, post-IR IRSL, MET-pIRIR.

1. Introduction

Luminescence dating can determine the time since commonly occurring natural minerals, such as quartz and feldspar, were last heated or exposed to sunlight, the so-called 'zeroing' events. The luminescence 'clock' is based on the time-dependent accumulation of electronic charge, generated by ambient radiation, at 'traps' in the crystal lattice of minerals, which is manifested by the measured intensity of thermoluminescence (TL) or optically stimulated luminescence (OSL). Since luminescence results from the recombination of electrons from traps with holes of luminescence centres, the observed luminescence intensity is not only controlled by the number of trapped electrons but also by the concentration of the luminescence centres or hole centres. The natural radiation dose received by the samples, or equivalent dose (D_e), is estimated by comparing the natural signals with laboratory-regenerated signals. However, a direct comparison between the natural and regenerative signals requires the sensitivity to be the same for the natural and regenerative signals, which is usually impossible as the sensitivity commonly varies after different laboratory treatments necessary for dating, such as laboratory dosing, preheating and stimulation (Stokes, 1994; Wintle and Murray, 1999; Blair et al., 2005). It is not until a single-aliquot regenerative-dose (SAR) protocol was proposed (Murray and Roberts, 1998; Galbraith et al., 1999; Murray and Wintle, 2000) that sensitivity changes caused by laboratory measurements for quartz OSL could be successfully allowed for. The SAR protocol was subsequently applied to the infrared stimulated luminescence (IRSL) dating of K-feldspars (Wallinga et al., 2000).

Quartz has been the main mineral used for optical dating of sediments over the last decade. However, the quartz OSL signal usually saturate at relatively low doses of ~200-400 Gy or even less and this has made it difficult to use for dating events before about 200 thousand years (ka) ago, unless the environmental dose rate is exceptionally low. Feldspars can also be used for optical dating, either using visible wavelengths for stimulation or using infrared stimulation to produce an IRSL signal (Hütt et al., 1988). The IRSL signal has been shown to continue to grow to higher dose levels than quartz OSL and, thus, it would be advantageous to develop a method that is based on IRSL

measurements of feldspars. However, feldspars have long been known to exhibit 'anomalous' (athermal) fading of the trapped charges related to the IRSL signals (Spooner, 1992, 1994; Huntley and Lamothe, 2001; Huntley and Lian, 2006)—that is, the leakage of electrons from traps at a much faster rate than would be expected from kinetic considerations (Wintle, 1973).

Given the great potential of extending the age range of luminescence dating using feldspar, attempts have been made to correct for or to avoid the anomalous fading effect (Sanderson and Clark, 1994; Lamothe and Auclair, 1999; Huntley and Lamothe, 2001; Zhao and Li, 2002;Lamothe et al., 2003; Tsukamoto et al., 2006; Li et al., 2007, 2008). Huntley and Lamothe (2001) proposed a method to correct for anomalous fading, based on the measurement of the fading rate (g value) in terms of percentage loss per decade (Aitken, 1985). However, this correction method can only be applied to young samples that fall within the linear region of the dose response curves. For older samples, this method becomes unreliable due to the dose dependency of the anomalous fading rate (Huntley and Lamothe, 2001; Kars et al., 2008; Li and Li, 2008). It has also been shown that fading correction procedures are unreliable for some young samples (Li et al, 2008; Reimann et al. 2011).

Recent progress in understanding anomalous fading in feldspar has raised the prospect of isolating a non-fading IRSL component for the dating of Quaternary deposits containing feldspars. By first bleaching feldspar grains using IR photons at 50°C and then measuring the post-IR IRSL (pIRIR) signal at an elevated temperature (>200°C), it is possible to sample more distance trap recombination centre pairs that suffer least from fading (Thomsen et al., 2008; Buylaert et al., 2009; Thiel et al., 2011). Alternatively, the non-fading component can be identified by using a multiple-elevated-temperature (MET) stimulation procedure—the so-called MET-pIRIR protocol (Li and Li, 2011; 2012)—in which the feldspar grains are stimulated with IR at successively higher temperatures, from 50°C to 300°C. In these pIRIR and MET-pIRIR procedures, the basic structure of the SAR protocol is adopted, in which the sensitivity of the regenerative-dose signals (L_x) is monitored and corrected for by the corresponding test-dose signals (T_x). A characteristic saturation dose (D_0) of ~300-400 Gy is

usually observed for the high-temperature pIRIR or MET-pIRIR signals, which places an upper limit of dose measurement of ~1000 Gy (Li and Li, 2012). In this study, we aim to study the sensitivity change of the MET-pIRIR signals and their response to irradiation, sunlight bleaching and heating. We show that it is possible to develop a new dating method based on the dose dependence of the sensitivity of the MET-pIRIR signals.

2. Sample preparation and instrumental details

Six aeolian samples (Sm1, Sm3, Sm5, Sm6, Sm6' and Sm8) were examined in this study (Table 1). These samples were taken from the Shimao section (Sun et al., 1999) at the southeastern margin of the Mu Us Desert (37°28'-39°23' N and 106°10'-110°30' E) (Fig. 1). The Shimao section is a 76.7-m-thick aeolian sequence consisting of 40 alternating sand/loess/palaeosol layers (Fig. 2), which were deposited within the last ~580 ka (Sun et al., 1999). The alternating sand/loess/palaeosol layers reflect the waxing and waning of the East Asian Monsoon (Sun et al., 1999). A detailed description of the sequence is given by Sun et al. (1999). Previous reconstruction of the chronology of the Shimao sequence have been mainly based on stratigraphic comparisons of different sites in the Loess Plateau and on correlations of grain size and magnetic susceptibility curves to the orbitally tuned Baoji section (Ding et al., 1994). Based on this chronology for the Shimao section, its magnetic susceptibility record can be correlated well with the global marine oxygen isotopic record (Fig. 2). The validity of the correlation in the upper part of the section has been further tested by TL dating (Sun et al., 1998) and OSL dating of quartz, and by isochron dating of K-feldspars (Li et al., 2011). The six samples examined in this study were taken from sand layers (Fig. 2), and have geological ages (expected ages) of between ~9 and ~470 ka (Table 1). These sediment samples have been extensively studied previously (Li et al., 2007; 2011; Li and Li, 2008). They were chosen for this study because: 1) their ages are stratigraphically confined, spanning the last ~500 ka. Therefore, they have received different natural doses, from the linear region of the dose response curve to the nearly saturated part and, hence, are excellent case studies to examine the natural-dose dependency of luminescence

behaviours; 2) these samples have a similar geological source and, hence, have similar luminescence characteristics and burial conditions, including environmental dose rate, dose response curve, luminescence sensitivity and fading rate. As a consequence, the dose response and other luminescence characteristics of the younger samples are thought to be analogues for the early stages of burial of the older samples in the section (Li and Li, 2008), which provides an ideal profile to test new dating methods.

3. Experimental procedures and analytical facilities

The samples were prepared for IRSL analysis using routine procedures (Aitken, 1998). First, they were treated with HCl acid and H_2O_2 solution to remove carbonates and organic matter, respectively, and then dried and sieved to obtain grains of 90–125, 125–150, 150–180 and 180–212 μm in diameter (Table 1). The K-feldspar grains were separated from quartz and heavy minerals using a solution of sodium polytungstate with a density of 2.58 g/cm^3. The separated K-feldspar grains were immersed in 10% HF acid for 40 min to etch the surfaces of the grains and remove the outer, alpha-irradiated portions, and then rinsed in HCl acid to remove any precipitated fluorides. After drying, the etched K-feldspar grains were mounted as a monolayer on stainless steel discs of 9.8 mm diameter using "Silkospray" silicone oil as an adhesive. Grains covered the central ~5 mm diameter portion of each disc, corresponding to several hundred grains per aliquot.

IRSL measurements were made on an automated Risø TL-DA-20 reader equipped with IR diodes for stimulation (870 Δ 40 nm). The total IR power delivered to the sample position was ~135 mW/cm^2 (Bøtter-Jensen et al., 2000), and laboratory irradiations were carried out on the reader using a calibrated ^{90}Sr/^{90}Y beta source. IRSL signals were detected by an Electron Tubes Ltd 9235B photomultiplier tube fitted with Schott BG-39 and Corning 7-59 filters to restrict transmission to 320–480 nm. Each IRSL measurement was made for 100 s. At the start of each IRSL measurement, an 'IR-off' period of 10–50 s was applied to avoid any thermal lag effect and any significant interference from thermoluminescence (TL) for the MET-pIRIR signal at high temperatures (Fu et al., 2012).

Typical IRSL and MET-pIRIR decay curves for sample Sm8 are shown in Fig. 3. The measured signal was calculated as the sum of counts over the initial 10 s of each IR-on stimulation, with 'late light' subtraction (Aitken, 1998) of the background count rate over the final 10 s of each stimulation. We note that the IRSL and pIRIR intensities does not reach a constant level after 100 s of stimulation (Fig. 3), but continues to decay, so the subtracted background consists of 'dark' counts intrinsic to the photomultiplier tube, scattered incident photons, and IRSL associated with the eviction of electrons from traps that are sensitive to IR radiation at the chosen stimulation temperature.

4. Experimental details and results

4.1. Effect of thermal treatment on IRSL sensitivity

In this study, 'sensitivity' is defined as the luminescence intensity per unit dose, and hereafter is referred to as sensitivity. It can be monitored using the measured luminescence signal (either TL, IRSL or OSL) when an aliquot of grains was subjected to a fixed test dose, preheat and measurement procedure. Previous studies showed that a high-temperature heat treatment or TL measurement up to 450°C can reduce the IRSL sensitivity for K-feldspar (Richardson, 1994; Blair et al., 2005). Here, we further investigate the effect of thermal annealing on the sensitivity of the IRSL and MET-pIRIR signals for our samples.

Three single aliquot of Sm8 was first exposed to bleached by IR stimulation at 250°C for 200 s to evict all charges from the IR-sensitive traps giving rise to IRSL signals. The IRSL and MET-pIRIR sensitivities of the K-feldspar grains on this aliquot were then measured by applying a small test dose of ~5.5 Gy, followed by a preheat at 300 °C for 60 s, and then stimulation of the IRSL and MET-pIRIR signals sequentially at 50, 100, 150, 200 and 250 °C. Each of the IRSL and MET-pIRIR signals were measured for 100 s, after which the aliquot was cut-heated to annealing temperature T, before measurement of the sensitivity following the same sequence as mentioned above (i.e., test dose, preheat and MET-pIRIR measurements). This sensitivity measurement cycle was repeated 14 times by increasing T from 320 to 590 °C in steps of 30 °C. The normalised sensitivities of the IRSL and

MET-pIRIR signals, as manifested by the net test-dose signals, are plotted against the annealing temperature in Fig. 4. It shows that thermal annealing can significantly change the sensitivity of the IRSL and MET-pIRIR signals. The sensitivity of the MET-pIRIR signals is more dependent on the thermal treatment than is the sensitivity of the low-temperature (50 °C) IRSL signal, and heating to a high annealing temperature (up to 600 °C) can largely deplete the sensitivity of the former. For the 50°C IRSL signal, the sensitivity is depleted by ~50% at ~400 °C and then slightly increasing again above 400°C. In contrast, the MET-pIRIR signals at elevated temperatures show a large depletion in sensitivity as the annealing temperature is increased. Most of the depletion occurred in the first 5 cycles (from 300 to 440 °C). The percentage depletions in sensitivity for the 100, 150, 200 and 250 °C MET-pIRIR signals are ~73%, 78%, 78% and 91%, respectively. The sensitivity of the MET-pIRIR signals is then stable from ~450 to ~600 °C. For the 100°C MET-pIRIR signal, its sensitivity reaches a relatively stable level at 28% of the initial value at ~500°C and higher temperatures. For the 150 °C MET-pIRIR signal, a stable level at 18% of its initial value is reached at ~500 °C and above. For the 200 and 250 °C signals, stable levels at 15% and 6% of their initial signal intensities, respectively, are reached at ~530°C and above.

From Fig. 4, it appears that, for the 250°C MET-pIRIR signals, a high-temperature annealing of up to 600 °C may deplete most (>90%) of the hole centres that accumulated charge in nature. This means that the pre-dose 'memory' can be erased by a high-temperature treatment (~600 °C) for K-feldspar. To test this, we investigated the dose dependence of the signal sensitivity and the effect of high-temperature annealing on sensitivity. A single aliquot of Sm8 was first heated to 600 °C to evict all trapped charges in the IRSL and MET-pIRIR traps. The aliquot was then treated using the procedure outlined in Table 2. The aliquot was first given a regenerative dose (step 1) and preheated at 300 °C for 60 s (step 2). The regenerative signals (L_x) were then measured using a standard MET-pIRIR procedure (steps 3-7). After that, it was subjected to a small test dose of 5.5 Gy (step 8), preheated using the same conditions as previously (step 9), and followed by the same MET-pIRIR measurements (steps 10-14) to measure the test dose signals. We refer to the test dose signals obtained

in steps 10-14 as T1. After that, the same aliquot was heated to 600 °C again (step 15) to erase the dose memory and sensitivity information. This was followed by another cycle of test dose, preheat and IRSL measurements (steps 16-22). The test dose signals observed in steps 18-22 are termed T2. The procedure listed in Table 2 was repeated using four different regenerative doses: 220, 440, 770 and 1100 Gy. The change in sensitivity of different IRSL and MET-pIRIR signals during the measurement sequence can be monitored using the test dose signals, T1 and T2.

T1 and T2 are plotted in Fig. 5 as a function of the regenerative dose (or pre-dose) administered in step 1. There is a strong pre-dose dependence of T1, and the extent of the dependence shows a clear temperature trend for the IRSL and MET-pIRIR signals. The 50 °C IRSL signal ($T1_{(50°C)}$) shows the least increase with pre-dose, while the largest increase with pre-dose was observed for the highest-temperature MET-pIRIR signal (250 °C). In contrast, there is very little difference of T2 on pre-dose for all IRSL and MET-pIRIR signals, increasing only by ~10% from pre-doses of 220 Gy to 1100 Gy. This result suggests that the sensitivity of the test dose signals, especially the high-temperature pIRIR signals, is strongly dependent on the pre-dose received. And that such 'memory' of pre-dose can be largely erased by applying a high-temperature (e.g., 600 °C or higher) anneal.

A significant implication of the results in Fig. 4 and Fig. 5 is that, in addition to dating using electron traps, heated feldspar can also be dated using the luminescence sensitivity, which is related to the hole centres. Therefore, a 'pre-dose' technique can be developed for dating of heated feldspars. Such a 'pre-dose' technique for feldspar is similar to that developed for quartz (Zimmerman, 1971; Fleming, 1973), but the two minerals sensitise in opposite directions—that is, heating typically sensitises quartz but de-sensitises feldspar, and irradiation de-sensitises quartz but sensitises feldspar. Further investigations of the potential of this method for dating of heated feldspars are required but they are not within the scope of this study.

4.2. Effect of solar bleaching on the sensitivity of the IRSL and MET-pIRIR signals

Although it has been shown above that sensitivity changes or pre-dose information can be largely eliminated from feldspars by heating to a high temperature (e.g., ~600°C), a sedimentary material is unlikely to have had its traps emptied in nature by heating to such a high temperature. Instead of heating, the "zeroing event" for sediments is typically exposure to sunlight during transport. Therefore, it is important to study sensitivity change as a result of solar bleaching. Five groups of 3 aliquots of sample Sm8 were used for these experiments. Each group was bleached using a Dr Hönle solar simulator (model: UVACUBE 400) for periods of time ranging from 0 to 120 min. Each aliquot was then measured following steps 2-22 in Table 2, resulting in the measurement of three groups of IRSL and MET-pIRIR signals (i.e., L_x, T1 and T2). To compare T1 among the different groups, the signals need to be normalised appropriately to account for any inter-aliquot variations. Since T1 is thought to contain the 'memory' of the pre-dose received in nature, T2 was used to normalise inter-aliquot variation, because most of the pre-dose memory is erased by heating to 600 °C (Fig. 5). The value of L_x/T1 should, thus, represent the concentration of trapped electrons, and T1/T2 should represent the concentration of hole centres.

Fig. 6(a) shows L_x/T1 plotted a function of solar bleaching time. The reduction in L_x/T1 with bleaching time clearly shows that the IRSL and pIRIR traps are bleachable by sunlight. The higher the stimulation temperature used for MET-pIRIR measurement, the harder it becomes for the signals to be bleached (Fig. 6(a)). This result is consistent with the observation by Li and Li (2011). Fig. 6(b) shows T1/T2 as a function of solar bleaching time. It is interesting to note that the value of T1/T2 also decreases with solar bleaching time (Fig. 6(b)). In contrast to L_x/T1, however, there is little difference between the bleaching rates of the IRSL and MET-pIRIR signals, and they all reached a stable level at 50-60% of the initial sensitivity after being bleached for ~40 min. The data shown in Fig. 6(b) suggest that the sensitivity (T1) (or hole centres) can be depleted by solar bleaching. It should be noted that the value of T1, even after prolonged periods of solar bleaching, is still ~6-8 times the value of T2 for the various IRSL and MET-pIRIR signals. This indicates that a large pool of hole centres is still

available after bleaching—these hole centres are not bleachable by sunlight, but that they can be eliminated by heating the grains to a high temperature (e.g., 600 °C).

4.3. Natural-dose sensitivity dependence

It has been shown that the IRSL and MET-pIRIR signals (L_x/T1) from feldspars can be almostly eliminated by exposure to sunlight (Fig. 6(a)), but that their sensitivity can only be reduced by ~50% upon exposure to sunlight (Fig. 6(b)). During the transport of sediment, exposure to sunlight will partly reset the sensitivity or the 'light-senstive' hole centres in feldspars. After burial, these 'light-senstive' hole centres are expected to accumulate charges again, as a result of exposure to natural radiation. We can, thus, expect older samples to have a higher sensitivity than younger samples. To test this, samples of different ages from Shimao section were investigated. The expected ages of these samples, and the corresponding natural doses received by them are provided in Table 1. It is expected that the natural IRSL and MET-pIRIR signals (L_n) from these samples as a function of their natural doses can be used to creat a 'natural dose response curve (DRC)', because these samples share a similar geological source and have similar luminescence characteristics. Four to six aliquots of each sample were measured using the procedure outlined in Table 2. The sensitivity-corrected natural signals (L_n/$T1_n$) are plotted against the expected natural dose in Fig. 7(a), which shows that the L_n/$T1_n$ values from the different samples are in good stratigraphic order (i.e., their values increase with natural dose). Similar 'natural DRCs' were observed for the IRSL and MET-pIRIR signals at 50, 100, 150 and 200 °C, but a distinctively different natural DRC was observed for the 250 °C MET-pIRIR signal (Fig. 7(a)). Fig. 7(b) shows the normalised sensitivities of the natural IRSL and MET-pIRIR signals ($T1_n$/T2) as a function of the expected natural dose. Interestingly, a strong natural-dose dependence of the sensitivity ($T1_n$/T2) was observed with the extent of dependence increasing with stimulation temperature. The 50 °C IRSL signal ($T1_{(50°C)}$) shows the least increase in $T1_n$/T2 with natural dose, while the largest increase with natural dose was observed for the high-temperature MET-pIRIR signal at 250 ºC. This result suggests that the sensitivity of the natural MET-pIRIR signals, monitored by the test dose signals ($T1_n$), is strongly dependent on the pre-dose received by the

sedimentary feldspar grains even though they might have not been heated before burial. The data displayed in Fig. 7(b) confirm that sunlight bleaching can partly reset the hole centres giving rise to the IRSL and MET-pIRIR signals, and that the sensitivity measured for natural samples has a 'memory' of the pre-dose received after the most recent exposure to sunlight with the higher the temperature signals having a stronger memory than the lower-temperature signals.

4.4. Laboratory-dose dependence of sensitivity

To investigate whether the pre-dose dependence of sensitivity observed for natural samples is also present in laboratory-irradiated samples, 8 groups of 3 aliquots of sample Sm5 were bleached using the solar simulator for 90 min to remove the natural signals. Aliquots from different groups were then given different laboratory doses ranging from 0 to 2750 Gy. These aliquots were then measured using the procedure listed in Table 2 to obtain regenerative MET-pIRIR signals (L_x) and their sensitivities (T1 and T2). The measured data were used to construct regenerative dose-response curves (DRCs) for sensitivity-corrected MET-pIRIR signals (L_x/T1) and their sensitivities (T1/T2) at different stimulation temperatures (Fig. 8(a) and (b)).

In Fig. 8(a), the IRSL and MET-pIRIR signals show different shapes in their DRCs. The DRC of the 50°C IRSL shows the highest sensitivity. The MET-pIRIR signals at 100 and 150 °C have similar DRCs to each other, whereas the 200 and 250°C signals—the latter in particular—have lower sensitivity-corrected intensities. All of the data sets in Fig. 8(a) can be fitted using a single saturating exponential function (dashed lines), from which the characteristic saturation dose (D_0) values so obtained are summarised in Table 3 for the different signals. The D_0 value is highest for the IRSL signal measured at 50°C (~640 Gy) and gradually decreases with increasing stimulation temperature (from ~520 Gy at 100 °C to ~340 Gy at 250 °C). The characteristics of the DRCs of the MET-pIRIR signals in Fig. 8(a) are consistent with the previous observations of Li and Li (2011).

Compared to $L_x/T1$, the normalised sensitivities (T1/T2) of the different signals show the opposite pattern in terms of their growth with dose (Fig. 8(b)). A stronger dose dependence was observed for the signals measured at higher stimulation temperatures: for example, the sensitivity (T1/T2) of the 250 °C signal increased 3-fold from 0 Gy to 2750 Gy, whereas the sensitivity of the 50 °C signal increased by only ~60%. We calculated the D_0 values for the saturating exponential DRCs fitted to the data sets in Fig. 8(b) (dashed lines) and these are summarised in Table 3. The D_0 values span a much narrower range (from ~670 to ~770 Gy) than the $L_x/T1$ D_0 values, and are consistent with each other at 1σ (Table 3). The dependency of stimulation temperature on D_0 seen in Fig. 8(a) is, thus, not observed in Fig. 8(b). These results indicate that the same group of hole centres are probably responsible for the signals measured at the different stimulation temperatures, and that these hole centres saturate at a higher dose than the electron traps associated with the IRSL and MET-pIRIR signals.

We also investigated the dose-dependent sensitivity of the two-step pIRIR signal measured at 290 ºC (Thiel et al., 2011) using the same sample and a similar procedure of that outlined in Table 2, but with the MET measurements replaced by a two-step IR stimulation procedure. This consisted of an initial IR stimulation at 50 ºC for 200 s, followed by a further IR stimulation at 290 ºC for 200 s. The resulting Lx/T1 and T1/T2 values for the pIRIR 290 ºC signal are plotted in Fig. 8 (a) and (b) (black circles). It can be seen that the dose dependence of the sensitivity of the pIRIR 290 ºC signal is much less than that of the MET-pIRIR 250 ºC signal, which implies that the pIRIR 290 ºC signal may involve different group of recombination centres from the case for the MET-pIRIR 250 ºC signal. The MET-pIRIR method, therefore, has an advantage over the two-step pIRIR method of being able to exploit the dose-dependency of the sensitivity for long-range dating.

The results in Fig. 7 and Fig. 8 allow comparisons of the natural DRCs and regenerative DRCs for the various signals, which are shown in Fig. 9(a-e). Fig. 9(a) shows that the natural DRC of the 50 °C IRSL signal is suppressed relative to the laboratory DRC. If the natural intensity is

projected onto the laboratory DRC, a significant dose underestimation is obtained, indicating anomalous fading of this signal. A similar pattern was observed for the 100 °C MET-pIRIR signal (Fig. 9(b)), with less underestimation for older samples (i.e., the higher doses), suggesting less anomalous fading of the 100 °C MET-pIRIR signal. This finding is consistent with the observations of Li and Li (2011, 2012). For the 150 °C MET-pIRIR signal (Fig. 9(c)), the natural data aligns more closely with the laboratory DRC, and the natural DRCs of the 200 and 250 °C MET-pIRIR signals are indistinguishable from their respective laboratory DRCs (Fig. 9(d) and (e)), indicating negligible anomalous fading of these signals. We note that, however, a slight underestimation in the 200 °C MET-pIRIR signal is still observed for the oldest sample Sm8 (~1600 Gy) (Fig. 9(d)), which is further reduced for the 250 °C MET-pIRIR signal (Fig. 9(e)).

In Fig. 10, the natural and laboratory DRCs of the normalised sensitivity (T1/T2) of the different signals were compared. Similar patterns to those in Fig. 9 can be observed (Fig. 10a-e). Most of the natural data sets were underestimated for the sensitivity of 50 °C IRSL signal (Fig. 10(a)). This indicates that the hole centres associated with the 50 °C IRSL signal also suffer from anomalous fading. However, the discrepancy between the natural and laboratory DRCs (i.e., the extent of underestimation in natural data sets) for the different MET-pIRIR signals decreases with increasing stimulation temperature (Fig. 10(b-e)). Consistent natural and laboratory DRCs were obtained for the 200 and 250 °C MET-pIRIR signals (Fig. 10(d) and 9(e)), indicating that the hole centres associated with these high-temperature MET-pIRIR signals suffer negligible from anomalous fading.

The extent of anomalous fading of the signal sensitivity (T1/T2) was further tested using a simple laboratory fading test. Two groups of five aliquots of sample Sm8 were bleached using the solar simulator for 90 min to remove their natural light-sensitive signals and also to partly reset their sensitivities. Each aliquot was then given a laboratory dose of 1100 Gy. One group of aliquots was immediately measured using the procedure outlined in Table 2, and the other group was stored in the dark for 40 days before being measured in the same way. The time difference between the delayed

measurements of the two groups is ~2.8 decades (i.e., a prompt measurement at ~100 min and a delayed measurement after 40 days). The ratios of L_x/T1 and T1/T2 between the delayed and prompt measurements are shown in Fig. 11. For L_x/T1, a 6% underestimation in the delayed measurement compared to the prompt was observed for the 50 °C IRSL signal. However, the delayed and prompt measurements yielded indistinguishable L_x/T1 ratios at higher stimulation temperatures. In contrast, no clear trend can be observed for the T1/T2 ratios calculated from the delayed and prompt measurements (Fig. 11). We note that these ratios are individually consistent with unity at 2σ, but the mean ratios are systematically higher by a few percent. This is probably due to large inter-aliquot variation among multiple aliquots. We also note that there is no underestimation in the delayed dose recovery test observed for the low-temperature signals (Fig. 11), despite an observed underestimation of T1/T2 for low temperature IRSL signals (e.g. 50 °C IRSL, Fig. 8(b)), which is likely indicative of fading in the IRSL signals related to T1.. This contradiction may be due to there being a greater rate of anomalous fading in natural samples, which is strongly dependent on the natural dose, compared to laboratory-irradiated samples (Huntley and Lian, 2006; Li and Li, 2008). The laboratory fading characteristics of the T1/T2 signals require further investigation using single aliquots but this is beyond the scope of this study.

Fig. 9 and 10 show that T1/T2 (i.e., hole centres) has a higher saturation dose level, but a significantly larger uncertainty (shown as vertical error bars in Fig. 10), compared to L_x/T1 (i.e., trapped electrons). The latter is especially pronounced for young samples, which suggests that L_x value is much more reproducible than its sensitivity (T1), presumably due to the much larger dose-dependency of the trapped electrons (L_x) compared to that of the hole centres (T1). To utilise both the high precision and reproducibility of L_x/T1 and the high characteristic saturation dose of T1/T2, we explored the possibility that L_x/T2 might provide an effective means of optimising precision and saturation dose. Fig. 12 compares the natural and laboratory DRCs of the normalised signal (L_x/T2) at different stimulation temperatures. As expected, the values of L_x/T2 have reduced uncertainties compared to T1/T2, especially for young samples. The saturation characteristics of L_x/T2 are similar

to those obtained for T1/T2, and are much higher than the saturation doses of L_x/T1 (Table 3). Instead of using T1/T2, therefore, we suggest that L_x/T2 may be more appropriate for dating of old samples, when L_x/T1 values fall in the saturated region of the DRC. It is noted that, for the low-temperature IRSL and pIRIR signals, more underestimation is observed in Lx/T2 (e.g. Fig. 12a) compared to Lx/T1 (Fig. 9a) and T1/T2 (Fig. 10a). This is expected because Lx/T2 is a multiplication of Lx/T1 and T1/T2, and the underestimation in both Lx and T1 will be multiplied to yield a larger underestimation.

4.5. Age estimation based on the new procedure

The regenerative DRCs of electron traps (L_x/T1) (Fig. 7) and hole centres (T1/T2) (Fig. 8) generated by the multiple-aliquot measurement procedure in Table 2 can be combined with measurements of the natural intensities to obtain D_e values and age estimates for the Shimao samples. This can be achieved for each of the DRCs in Fig. 9, 10 and 12. We have remarked earlier that the extent of anomalous fading is least of the higher stimulation temperatures, so we focus our attention here to the 250 ºC MET-pIRIR signal. The D_e values and ages given by this signal for L_x/T1, L_x/T2 and T1/T2 are summarised in Table 1. The ages from the L_x/T1 and L_x/T2 plotted against the expected ages, based on stratigraphic correlation, are summarized in Fig. 13(a) and (b), respectively. The L_x/T1 ratios give reliable ages of up to ~250 ka for the 250 ºC MET-pIRIR signal, but then underestimate the ages of the older samples Sm6' and Sm8 (Fig. 13a). The ages obtained for the two samples using L_x/T1 should be considered unreliable, because the natural signals are close to the saturation level (Fig. 9); any slight uncertainty in the measured value will result in a significant change in age. By contrast, reliable ages of up to ~500 ka can be obtained for all of the samples investigated when the 250ºC MET-pIRIR measurements of the L_x/T2 are used instead (Fig. 13(b)). This is expected because the natural doses measured are below, or close to, twice the the value of the characteristic saturation dose (D_0), which is sometimes considered a predicted upper limit for reliable D_e determination (Wintle and Murray, 2006; but see Galbraith and Roberts, 2012). The $2D_0$ value for the 250 ºC MET-pIRIR signal

is ~1500 Gy, which conservatively permits dating of samples deposited as far back as 500-750 ka ago at environmental dose rates of 2-3 ka/Gy.

5. Discussion

In the SAR protocol, sensitivity changes are monitored or measured using the signals induced by a test dose of fixed size. Two factors should be considered as causes of sensitivity change. One is the change in trapping probability during irradiation, caused by competition among different kinds of trap. A change in the relative proportion of non-bleachable and bleachable traps during a SAR measurement procedure may result in a change in the number of trapped electrons in the OSL/IRSL traps of interest when the test dose is given.

The other factor to consider is the change in recombination probability during OSL/IRSL stimulation, which is mainly controlled by the number of holes at luminescence centres and their abundance relative to non-radiative (or 'killer') centres. For the IRSL signals from K-feldspar, we observed a significant dependence of sensitivity on irradiation, heating and solar bleaching (Fig. 4, 5, 6 and 7). We attribute the dose dependence mainly to changes in the recombination probability during IRSL measurements, caused by changes in the number of hole centres, for the following reasons: 1) changes in trapping probability during irradiation due to competition among different kinds of trap are unlikely to cause such a significant dose dependence in sensitivity; for example, we observed a ~300% change in the sensitivity of the 250 ºC MET-pIRIR signal from 0 to ~2000 Gy (Fig. 8). This suggestion is supported by the modeling results of Kars and Wallinga (2009), who found that trapping probabilities during irradiation differed by less than ~30% between systems with and without trap competition. 2) The low-temperature IRSL and high-temperature MET-pIRIR signals differ significantly in their dose-dependent changes in sensitivity (e.g., Fig. 8). This difference cannot be explained by changes in trapping probabilities during irradiation, because trapping competition during irradiation should have a similar effect on all traps giving rise to the IRSL and MET-pIRIR signals. Instead, the differential sensitivity changes of the IRSL and MET-pIRIR signals can be explained by

the different recombination routes used during IR stimulation (Jain and Ankjaergaard, 2011; Li, 2010).

It has been suggested that the low-temperature IRSL signal is dominated by emissions from tunnelling recombination (Poolton et al., 2002), while the pIRIR signal is dominated by the emissions from thermally assisted recombination via the band-tail states or the conduction band (Jain and Ankjaergaard, 2011). In other words, low-temperature IRSL signal is dominated by localised recombination of electron-hole pairs, whereas the high-temperature pIRIR signals are mainly from delocalised recombination. The probability of localised recombination is determined mainly by the distance between electron-hole pairs (Huntley, 2006), and is less dependent on the number of recombination centres. In contrast, the probability of delocalised recombination should be more closely related to the number of recombination centres available. Therefore, we conclude that the dose dependent sensitivity of the high-temperature MET-pIRIR signals observed for our samples is mainly the result of changes in the number of hole centres.

The fact that the sensitivity of MET-pIRIR signals can be 'reset' by heating to a high temperature (Fig. 4) or to exposure to sunlight (Fig. 6) suggests that there is a large pool of distant hole centres shared by the high-temperature pIRIR traps and other luminescence (TL and OSL) traps. During heating and solar bleaching, the hole centres are depleted by recombination with electrons released from various TL and OSL traps. Then, when the sediments are re-buried, the number of holes begins to accumulate again. Therefore, the number of hole centres, manifested by the luminescence sensitivity of the sample, is also time-dependent and, hence, can be used for dating. Our results also imply that the traps associated with IRSL and MET-pIRIR signals represent only a minor fraction of the total pool of TL or OSL traps that can be stimulated by high-energy photons of sunlight or by heating to a high temperature. Therefore, the successive dosing and IRSL measurement cycles used in a SAR protocol for dating feldspar may potentially increase the number of IR-insensitive traps and, as a result, change the trapping probability between successive irradiations due to altered charge

competition. It is, thus, recommended that a solar bleaching step, or a 'hot' bleaching (such as a high-temperature IR or OSL bleach) equivalent to the effect of a solar bleach, be incorporated into the SAR procedure at the end of each test dose measurement to minimise the difference in trapping probabilities during natural and laboratory irradiation.

We have proposed a multiple-aliquot protocol for determining ages using the sensitivities of feldspar IRSL signals (e.g., T1/T2 or L_x/T2) as a practical method to extend the age range of feldspars. This method will be most suitable for old samples with homogeneous behaviours among grains. As shown in Fig. 4, 5 and 6, the sensitivity of K-feldspar grains is not only dependent on the natural dose received since their last exposure to sunlight, but is also dependent on their thermal history. For example, some grains may have been heated to a high temperature in a bushfire event before transportation to their final burial place, whereas other grains may not have been heated. This could result in significant grain-to-grain variation in sensitivity and, hence, aliquot-to-aliquot variation. In such cases, the multiple-aliquot method may not be applicable and development of a single-aliquot method is necessary. The latter could be achieved by incorporating multiple solar bleaching steps into a SAR procedure, but this requires further investigations of the effect of multiple treatments of solar bleaching and preheating on signal sensitivity. Detailed studies of the feasibility of developing a single-aliquot protocol are currently underway, but they are beyond the scope of this study, which lays the foundation for exploiting dose-dependent sensitivity changes in K-feldspar as a new Quaternary chronometer.

6. Conclusions

A dose-dependent luminescence behaviour—that is the sensitivity of the MET-pIRIR signal measured at elevated temperature (e.g., 250 ºC)—has been reported for K-feldspar. This phenomenon can potentially extend the age range of luminescence dating using K-feldspar, but it is premature to expect that accurate ages can be obtained routinely for all samples from different locations, given that a multiple-aliquot method has been proposed, which requires homogeneous behaviour among grains

and aliquots. For the samples examined from the Shimao section in China, dating using the dose-dependent sensitivity is best suited to 'old' samples, with natural doses higher than ~1000 Gy. At such doses, the pIRIR signals (Lx/T1), currently preferred for IRSL dating (Li and Li, 2011a), are saturated. For younger samples, the latter signals are preferred because of the much smaller uncertainties in Lx/T1 compared to those obtained for the sensitivity (T1/T2) (Fig. 9 and 10) and because of their suitability for single-aliquot measurements. The development of single-aliquot and single-grain methods based on the dose dependent sensitivity of the MET-pIRIR signals would provide a chronometer of comparable accuracy and precision, applicable to a much broader time range than can currently be dated using K-feldspar or quartz.

Acknowledgements

We thank Dr. Tony Reimann and another anonymous reviewer for providing valuable comments on the manuscript. This study was supported by a University of Wollongong Vice-Chancellor's Postdoctoral Research Fellowship to Li, by Australian Research Council grants and fellowships to Roberts (DP0880675) and Jacobs (DP1092843), and by the Research Grant Council of the Hong Kong Special Administrative Region, China, to SHL (7028/08P).

References

Adamiec, G., Aitken, M.J., 1998. Dose-rate conversion factors: update. Ancient TL 16, 37-50.

Aitken, M.J., 1985. Thermoluminescence Dating. Academic Press, London.

Aitken, M.J., 1998. An Introduction to Optical Dating. Oxford University Press, Oxford.

Blair, M.W., Yukihara, E.G., McKeever, S.W.S., 2005. Experiences with single-aliquot OSL procedures using coarse-grain feldspars. Radiation Measurements 39, 361-374.

Bøtter-Jensen, L., Bulur, E., Duller, G.A.T., Murray, A.S., 2000. Advances in luminescence instrument systems. Radiation Measurements 32, 523-528.

Buylaert, J.P., Murray, A.S., Thomsen, K.J., Jain, M., 2009. Testing the potential of an elevated temperature IRSL signal from K-feldspar. Radiation Measurements 44, 560-565.

Ding, Z., Yu, Z., Rutter, N.W., Liu, T., 1994. Towards an orbital time-scale for Chinese loess deposits. Quaternary Science Reviews 13, 39-70.

Fleming, S.J., 1973. The pre-dose technique: a new thermoluminescence dating method. Archaeometry 15, 13-30.

Fu, X., Li, B., Li, S.H., 2012. Testing a multi-step post-IR IRSL dating method using polymineral fine grains from Chinese loess. Quaternary Geochronology 10, 8-15.

Galbraith, R.F., Roberts, R.G., Laslett, G.M., Yoshida, H., Olley, J.M., 1999. Optical dating of single and multiple grains of quartz from Jinmium rock shelter, northern Australia, part 1, Experimental design and statistical models. Archaeometry 41, 339-364.

Galbraith, R.F., Roberts, R.G., 2012. Statistical aspects of equivalent dose and error calculation and display in OSL dating: An overview and some recommendations. Quaternary Geochronology 11, 1-27.

Huntley, D.J., 2006. An explanation of the power-law decay of luminescence. Journal of Physics-Condensed Matter 18, 1359-1365.

Huntley, D.J., Baril, M.R., 1997. The K content of the K-feldspars being measured in optical dating or in thermoluminescence dating. Ancient TL 15, 11-13.

Huntley, D.J., Hancock, R.G.V., 2001. The Rb contents of the K-feldspars being measured in optical dating. Ancient TL 19, 43-46.

Huntley, D.J., Lamothe, M., 2001. Ubiquity of anomalous fading in K-feldspars and the measurement and correction for it in optical dating. Canadian Journal of Earth Sciences 38, 1093-1106.

Huntley, D.J., Lian, O.B., 2006. Some observations on tunnelling of trapped electrons in feldspars and their implications for optical dating. Quaternary Science Reviews 25, 2503-2512.

Hütt, G., Jaek, I., Tchonka, J., 1988. Optical dating: K-feldspars optical response stimulation spectra. Quaternary Science Reviews 7, 381-385.

Jain, M., Ankjaergaard, C., 2011. Towards a non-fading signal in feldspar: insight into charge transport and tunnelling from time-resolved optically stimulated luminescence. Radiation Measurements 46, 292-309.

Kars, R.H., Wallinga, J., 2009. IRSL dating of K-feldspars: modelling natural dose response curves to deal with anomalous fading and trap competition. Radiation Measurements 44, 594-599.

Kars, R.H., Wallinga, J., Cohen, K.M., 2008. A new approach towards anomalous fading correction for feldspar IRSL dating - tests on samples in field saturation. Radiation Measurements 43, 786-790.

Lamothe, M., Auclair, M., 1999. A solution to anomalous fading and age shortfalls in optical dating of feldspar minerals. Earth and Planetary Science Letters 171, 319-323.

Lamothe, M., Auclair, M., Hamzaoui, C., Huot, S., 2003. Towards a prediction of long-term anomalous fading of feldspar IRSL. Radiation Measurements 37, 493-498.

Li, B., 2010. The relationship between thermal activation energy, infrared stimulated luminescence and anomalous fading of K-feldspars. Radiation Measurements 45, 757-763.

Li, B., Li, S.H., 2008. Investigations of the dose-dependent anomalous fading rate of feldspar from sediments. Journal of Physics D-Applied Physics 41, 225502.

Li, B., Li, S.H., 2011. Luminescence dating of K-feldspar from sediments: A protocol without anomalous fading correction. . Quaternary Geochronology 6, 468-479.

Li, B., Li, S.H., 2012. Luminescence dating of Chinese loess beyond 130 ka using the non-fading signal from K-feldspar. Quaternary Geochronology 10, 24-31.

Li, B., Li, S.H., Sun, J.M., 2011. Isochron dating of sand-loess-soil deposits from the Mu Us Desert margin, central China. Quaternary Geochronology 6, 556-563.

Li, B., Li, S.H., Wintle, A.G., Zhao, H., 2007. Isochron measurements of naturally irradiated K-feldspar grains. Radiation Measurements 42, 1315-1327.

Li, B., Li, S.H., Wintle, A.G., Zhao, H., 2008. Isochron dating of sediments using luminescence of K-feldspar grains. Journal of Geophysical Research-Earth Surface 113, F02026.

Murray, A.S., Roberts, R.G., 1998. Measurement of the equivalent dose in quartz using a regenerative-dose single-aliquot protocol. Radiation Measurements 29, 503-515.

Murray, A.S., Wintle, A.G., 2000. Luminescence dating of quartz using an improved single-aliquot regenerative-dose protocol. Radiation Measurements 32, 57-73.

Poolton, N.R.J., Wallinga, J., Murray, A.S., Bulur, E., Bøtter-Jensen, L., 2002. Electrons in feldspar I: on the wavefunction of electrons trapped at simple lattice defects. Physics and Chemistry of Minerals 29, 210-216.

Richardson, C.A., 1994. Effects of bleaching on the sensitivity to dose of the infrared stimulated luminescence of potassium-rich feldspars from Ynyslas, Wales. Radiation Measurements 23, 587-591.

Sanderson, D.C.W., Clark, R.J., 1994. Pulsed photostimulated luminescence of alkali feldspars. Radiation Measurements 23, 633-639.

Spooner, N.A., 1992. Optical dating: preliminary results on the anomalous fading of luminescence from feldspars. Quaternary Science Reviews 11, 139-145.

Spooner, N.A., 1994. The anomalous fading of infrared-stimulated luminescence from feldspars. Radiation Measurements 23, 625-632.

Stokes, S., 1994. The timing of OSL sensitivity changes in a natural quartz. Radiation Measurements 23, 601-605.

Sun, J.M., Ding, Z.L., Liu, T.S., Rokosh, D., Rutter, N., 1999. 580,000-year environmental reconstruction from aeolian deposits at the Mu Us Desert margin, China. Quaternary Science Reviews 18, 1351-1364.

Sun, J.M., Yin, G.M., Ding, Z.L., Liu, T.S., Chen, J., 1998. Thermoluminescence chronology of sand profiles in the Mu Us Desert, China. Palaeogeography, Palaeoclimatology, Palaeoecology 144, 225-233.

Thiel, C., Buylaert, J.P., Murray, A., Terhorst, B., Hofer, I., Tsukamoto, S., Frechen, M., 2011. Luminescence dating of the Stratzing loess profile (Austria) - testing the potential of an elevated temperature post-IR IRSL protocol. Quaternary International 234, 23-31.

Thomsen, K.J., Murray, A.S., Jain, M., Botter-Jensen, L., 2008. Laboratory fading rates of various luminescence signals from feldspar-rich sediment extracts. Radiation Measurements 43, 1474-1486.

Tsukamoto, S., Denby, P.M., Murray, A.S., Bøtter-Jensen, L., 2006. Time-resolved luminescence from feldspars: new insight into fading. Radiation Measurements 41, 790-795.

Wallinga, J., Murray, A., Wintle, A., 2000. The single-aliquot regenerative-dose (SAR) protocol applied to coarse-grain feldspar. Radiation Measurements 32, 529-533.

Wintle, A.G., 1973. Anomalous fading of thermoluminescence in mineral samples. Nature 245, 143-144.

Wintle, A.G., Murray, A.S., 1999. Luminescence sensitivity changes in quartz. Radiation Measurements 30, 107-118.

Wintle, A.G., Murray, A.S., 2006. A review of quartz optically stimulated luminescence characteristics and their relevance in single-aliquot regeneration dating protocols. Radiation Measurements 41, 369-391.

Zhao, H., Li, S.H., 2002. Luminescence isochron dating: a new approach using different grain sizes. Radiation Protection Dosimetry 101, 333-338.

Zhao, H., Li, S.H., 2005. Internal dose rate to K-feldspar grains from radioactive elements other than potassium. Radiation Measurements 40, 84-93.

Zimmerman, J., 1971. The radiation-induced increase of the 100 °C thermoluminescence sensitivity of fired quartz. Journal of Physics C: Solid State Physics 4, 3265-3276.

Figure captions

Figure 1: Map showing the Mu Us Desert and the Shimao section.

Figure 2: Sample locations, stratigraphy, and magnetic susceptibility (MS) curve for the Shimao section, together with SPECMAP oxygen isotope curve for the last 550 ka. The oxygen isotope stages are numbered and the interglacial periods are shaded. Note the different units on the y-axis of the MS curve (depth) and the SPECMAP curve (age).

Figure 3: Typical IRSL and MET-pIRIR signals from sample Sm8 measured at different stimulation temperatures.

Figure 4: The sensitivities of the IRSL and MET-pIRIR signals plotted against the annealing temperature. The sensitivities were calculated based on the intensities of the test dose signals, and are plotted (normalised) relative to the initial sensitivity of each signal at the annealing temperature of 300 °C.

Figure 5: Test dose signals, T1 and T2, as a function of regenerative dose (or pre-dose). The stimulation temperature of the signals is shown inside the brackets following T1 and T2 in the legend. All data sets are normalised to unity at 220 Gy.

Figure 6: L_x/T1 (a) and T1/T2 (b) as a function of solar bleaching time. Each data point represents the average of 3 aliquots and error bars are shown when larger than the size of the symbol. Bleaching was conducted using a Dr Hönle solar simulator (model: UVACUBE 400) and the measurements were made following steps 2-22 in Table 2.

Figure 7: Values of L_n/T1 (a) and $T1_n$/T2 (b) obtained from natural samples plotted against the expected natural dose (Table 1). The data sets were obtained using the procedure shown in Table 2. Each data point represents the average of 4-6 aliquots for each sample, and the error bars are shown when lager than the size of the symbol.

Figure 8: Values of L_x/T1 (a) and T1/T2 (b) obtained from laboratory-irradiated samples plotted against the laboratory dose. Each data point represents the average of 4-6 aliquots of Sm5. The aliquots were bleached

for 90 min using a solar simulator to empty the natural signals before measurement using the procedure in Table 2. The data for the various signals were fitted using a single saturating exponential function (dashed lines). The characteristic saturation dose (D_0) values for these signals are summarised in Table 3.

Figure 9: Comparisons of the natural and laboratory-regenerated DRCs for the sensitivity-corrected IRSL and MET-pIRIR signals (Lx/T1). The dashed lines represent the least-squares fits to the regenerative signals using a single saturating exponential function. The vertical error bars are smaller than the size of the symbols. The data sets are taken from Fig. 7(a) and 8(a).

Figure 10: Comparisons of the natural and laboratory-regenerated DRCs constructed for the normalised sensitivities (T1/T2) of the IRSL and various MET-pIRIR signals. The dashed lines are single saturating exponential functions fitted to the regenerative-dose data. The data sets are taken from Fig. 7(b) and 8(b).

Figure 11: The ratio of the values of L_x/T1 (red squares) and T1/T2 (blue diamonds) measured with and without a delay after laboratory irradiation; the latter is referred to as the prompt measurement. The results were obtained using two groups of aliquots of Sm8, which were first bleached using the solar simulator for 90 min and then given a laboratory dose of 1100 Gy. One group was then promptly measured using the procedure in Table 2, and the other group was stored in darkness for 40 days before measurement. The time difference between the measurements of the two groups of aliquots is ~2.8 decades.

Figure 12: Comparisons of the natural and laboratory-regenerated DRCs of the normalised sensitivities (Lx/T2) for the IRSL and different MET-pIRIR signals. The dashed lines are single saturating exponential functions fitted to the regenerative-dose data. Each data point represents the average of 4-6 aliquots.

Figure 13: Comparisons of the ages for all samples obtained using Lx/T1 (a) and Lx/T2 (b) and the expected ages based on stratigraphic correlation. The Lx/T1 and Lx/T2 ages were obtained by projecting the natural intensities onto the DRCs in Fig. 9 and Fig. 12, respectively.

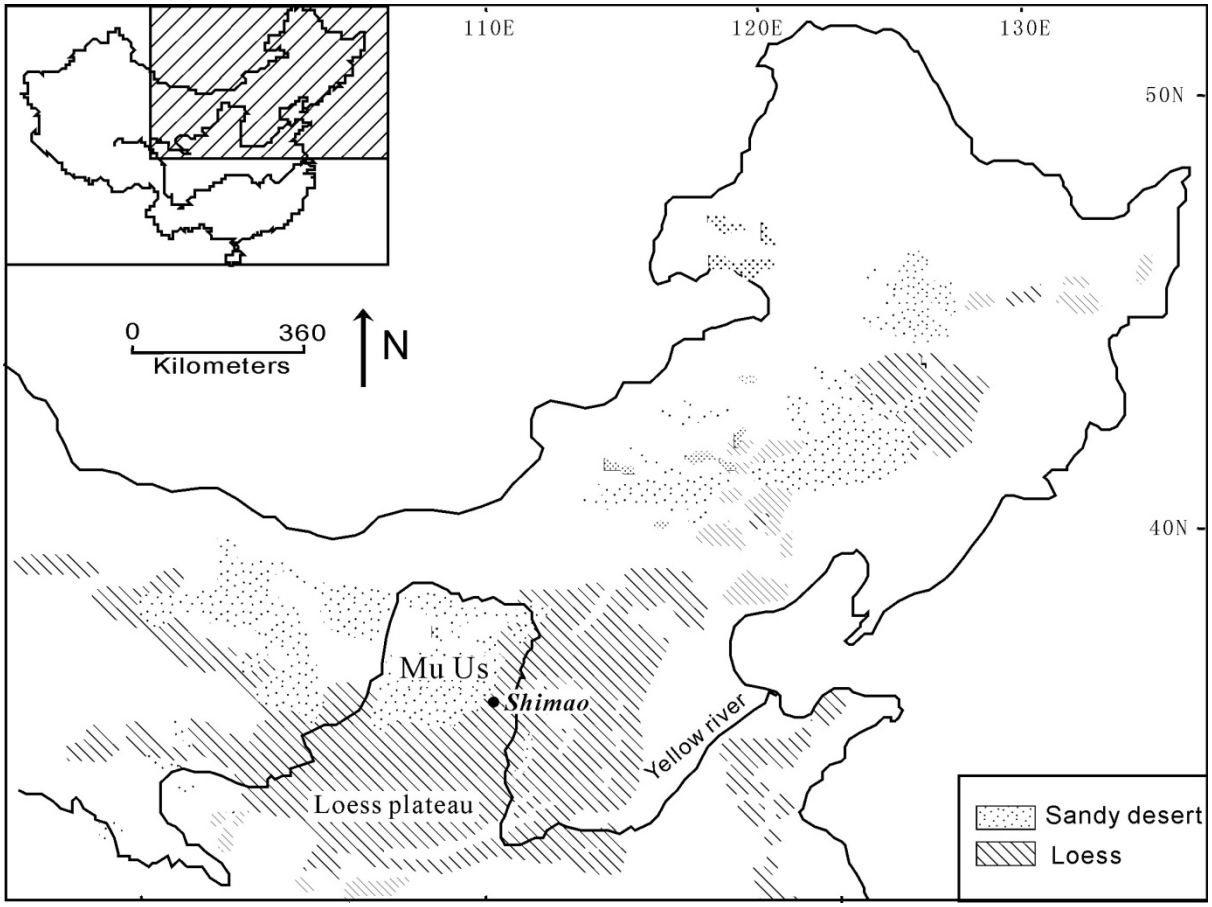
110E
120E
130E
50N
40N
0
360
Kilometers
N
Mu Us
Shimao
Yellow river
Loess plateau
Sandy desert
Loess

Figure 1

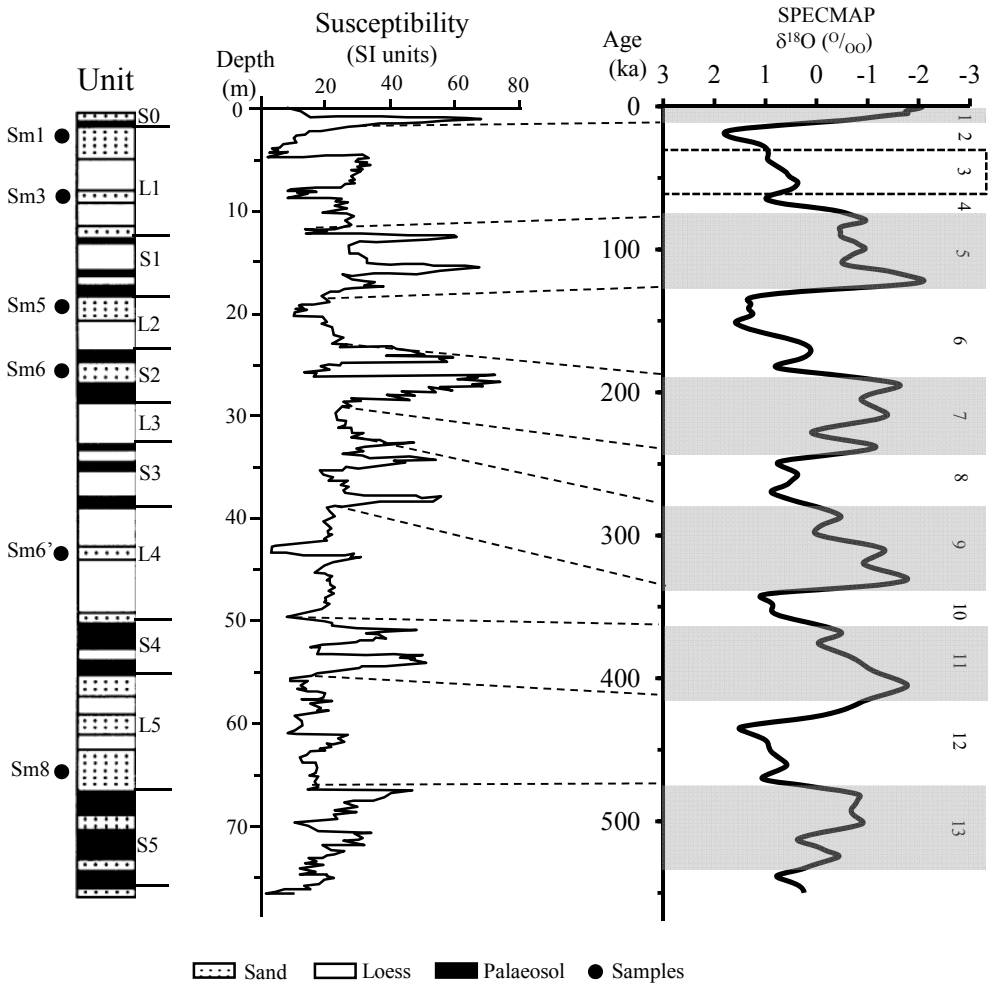
Unit
Depth (m)
Susceptibility (SI units)
20
40
60
80
Age (ka)
SPECMAP δ18O (‰)
3
2
1
0
-1
-2
-3
0
10
20
30
40
50
60
70
100
200
300
400
500
S0
L1
S1
L2
S2
L3
S3
L4
S4
L5
S5
Sm1
Sm3
Sm5
Sm6
Sm6'
Sm8
1
2
3
4
5
6
7
8
9
10
11
12
13
Sand
Loess
Palaeosol
Samples

Figure 2

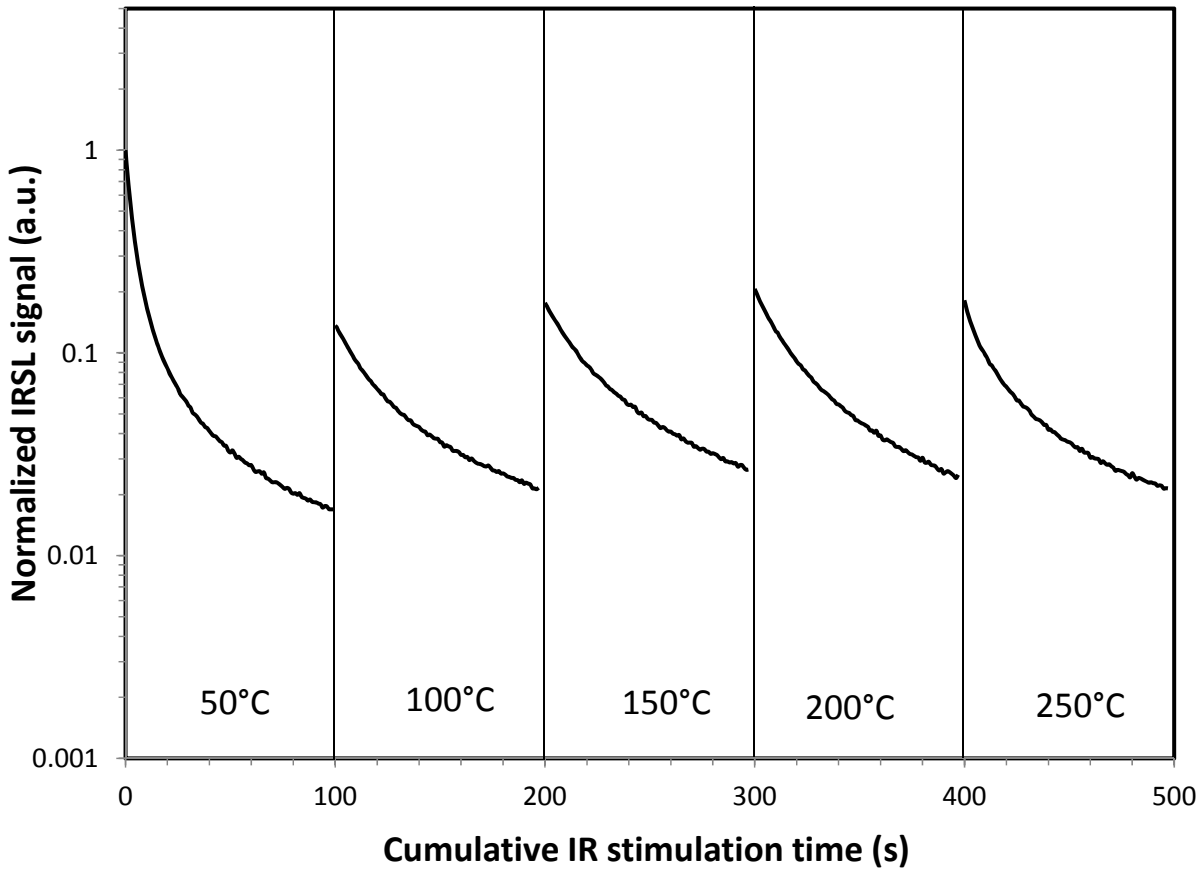
Normalized IRSL signal (a.u.)
1
0.1
0.01
0.001
50°C
100°C
150°C
200°C
250°C
0
100
200
300
400
500
Cumulative IR stimulation time (s)

Figure 3

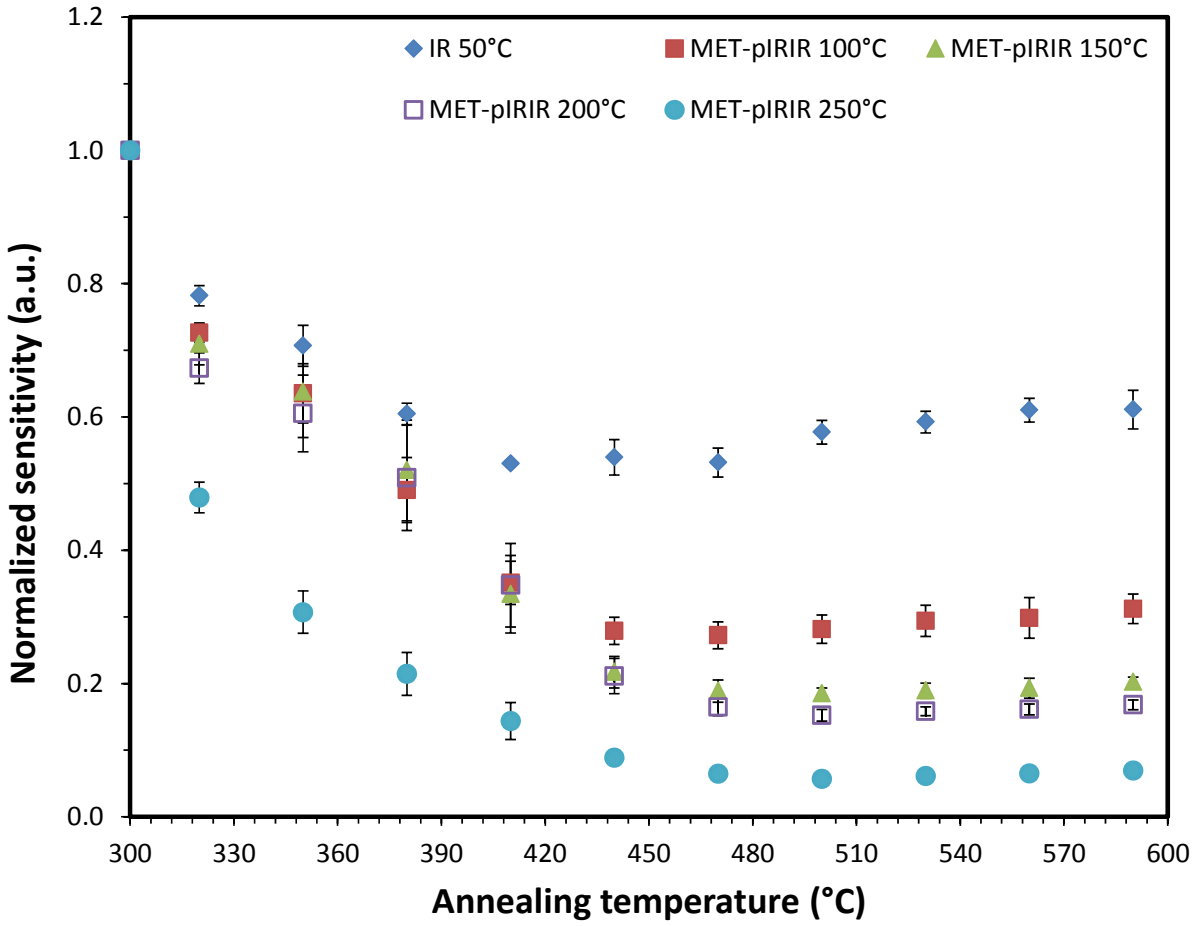
IR 50°C
MET-pIRIR 100°C
MET-pIRIR 150°C
MET-pIRIR 200°C
MET-pIRIR 250°C
Normalized sensitivity (a.u.)
1.2
1.0
0.8
0.6
0.4
0.2
0.0
300
330
360
390
420
450
480
510
540
570
600
Annealing temperature (°C)

Figure 4

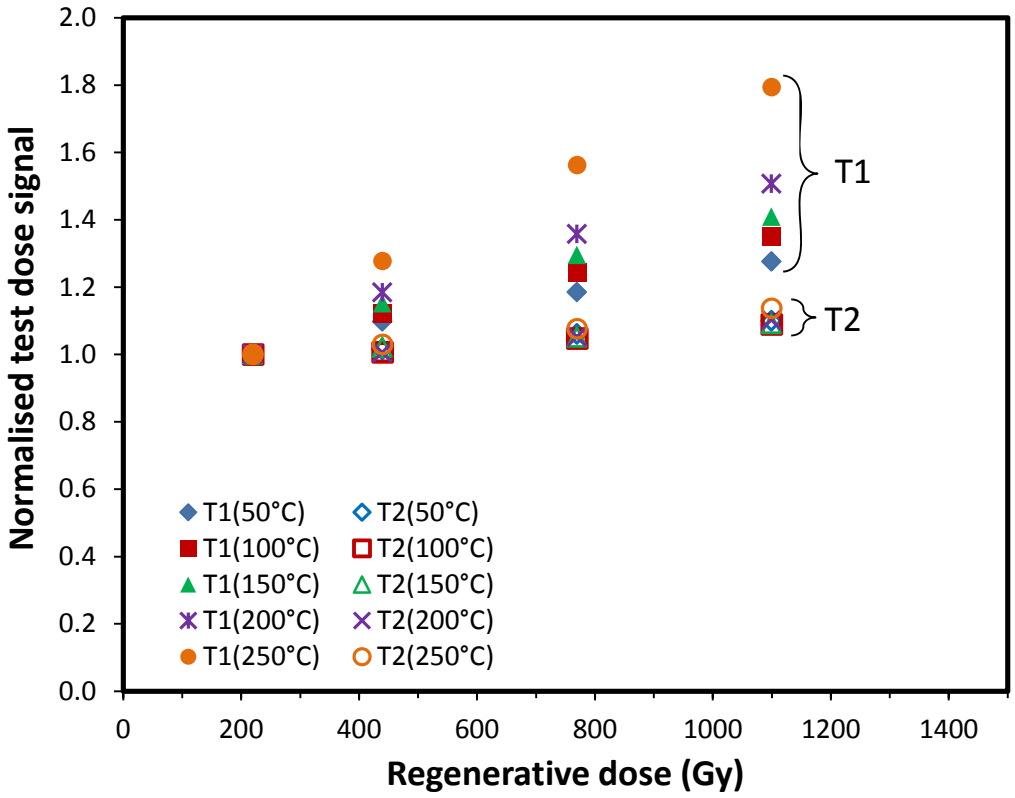
Normalised test dose signal
Regenerative dose (Gy)
2.0
1.8
1.6
1.4
1.2
1.0
0.8
0.6
0.4
0.2
0.0
0
200
400
600
800
1000
1200
1400
T1
T2
T1(50°C)
T2(50°C)
T1(100°C)
T2(100°C)
T1(150°C)
T2(150°C)
T1(200°C)
T2(200°C)
T1(250°C)
T2(250°C)

Figure 5

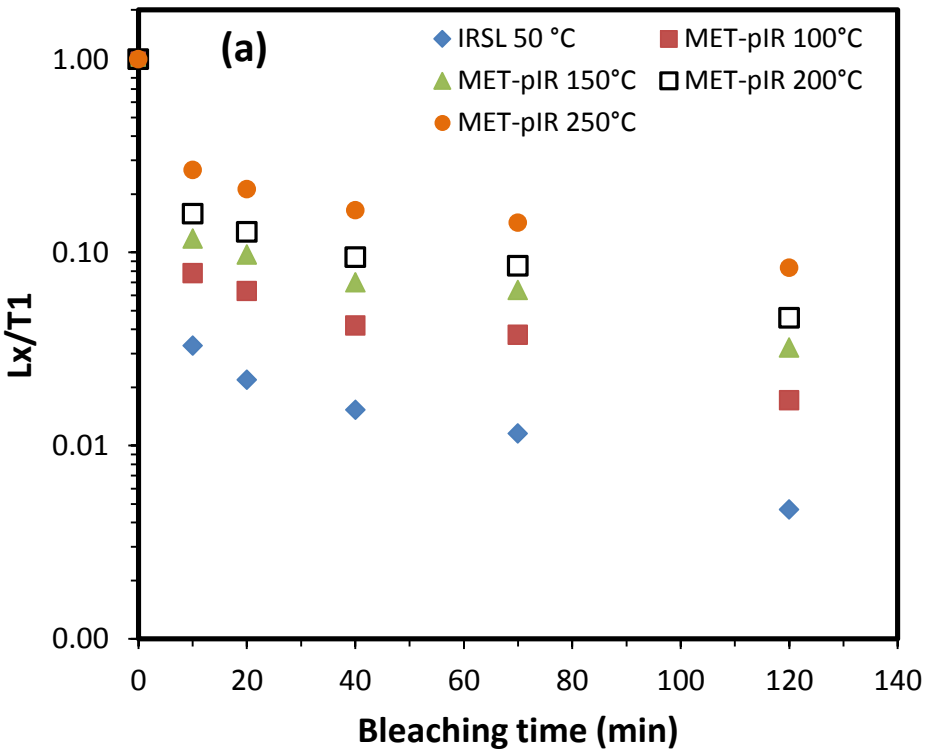
(a)
IRSL 50 °C
MET-pIR 100°C
MET-pIR 150°C
MET-pIR 200°C
MET-pIR 250°C
Lx/T1
1.00
0.10
0.01
0.00
0
20
40
60
80
100
120
140
Bleaching time (min)

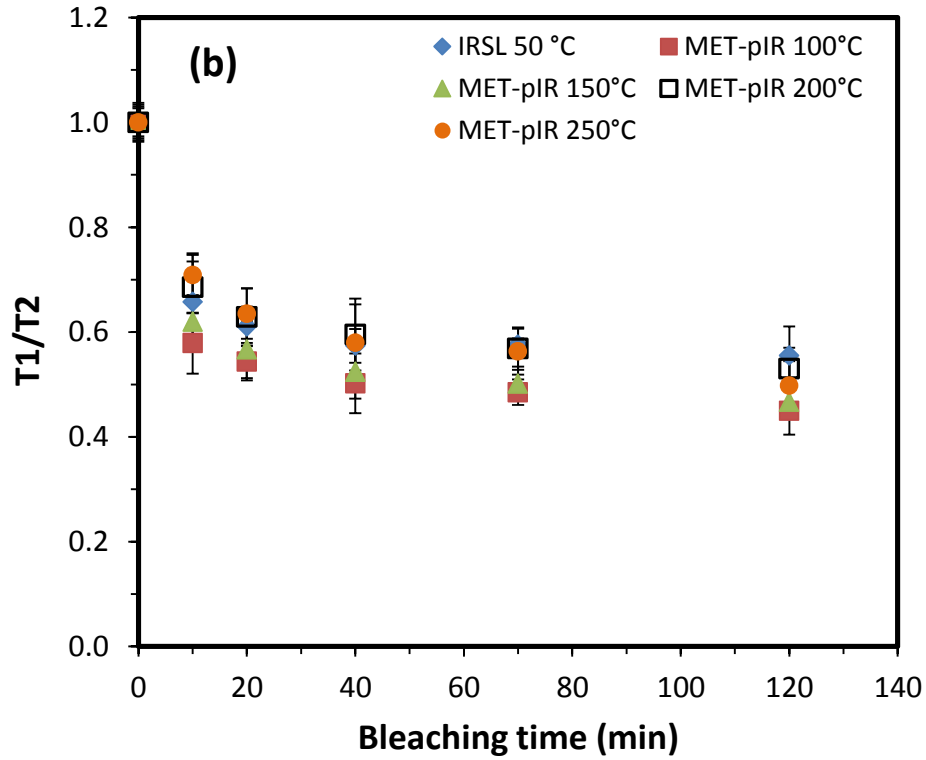
(b)
IRSL 50 °C
MET-pIR 100°C
MET-pIR 150°C
MET-pIR 200°C
MET-pIR 250°C
T1/T2
1.2
1.0
0.8
0.6
0.4
0.2
0.0
0
20
40
60
80
100
120
140
Bleaching time (min)

Figure 6

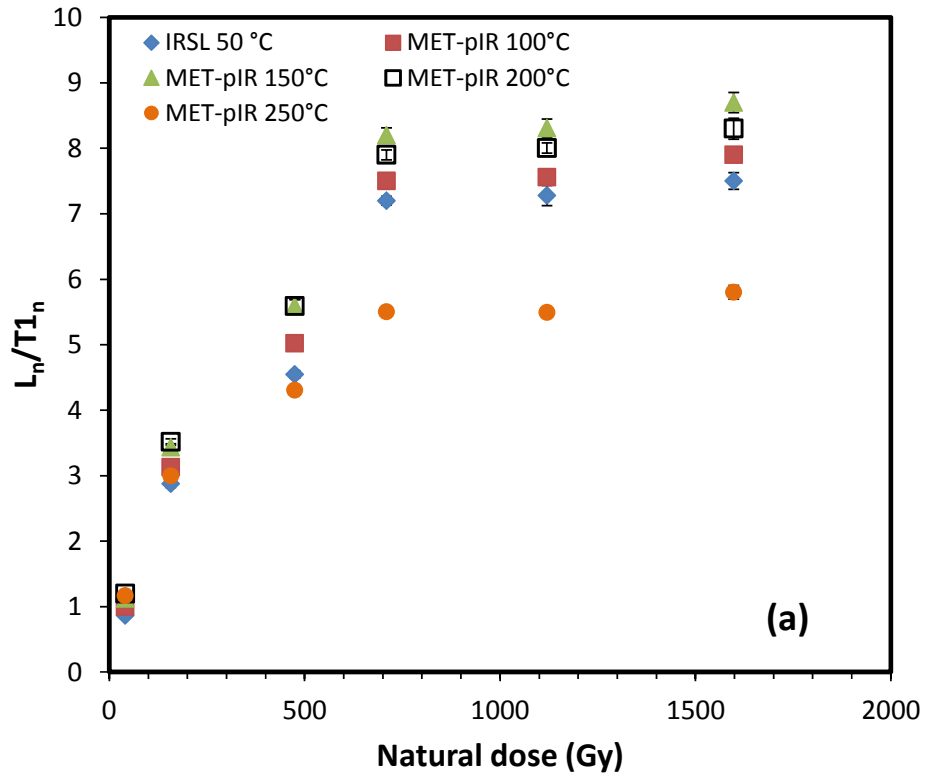
IRSL 50 °C
MET-pIR 100°C
MET-pIR 150°C
MET-pIR 200°C
MET-pIR 250°C
$L_n/T1_n$
Natural dose (Gy)
(a)

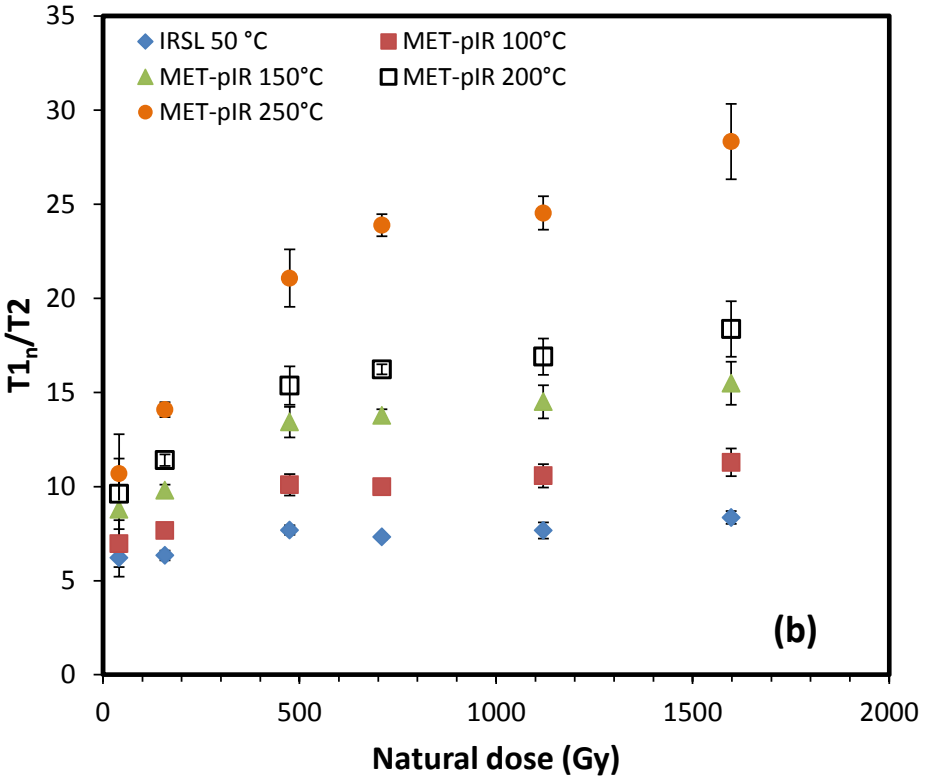
IRSL 50 °C
MET-pIR 100°C
MET-pIR 150°C
MET-pIR 200°C
MET-pIR 250°C
$T1_n/T2$
Natural dose (Gy)
(b)

Figure 7

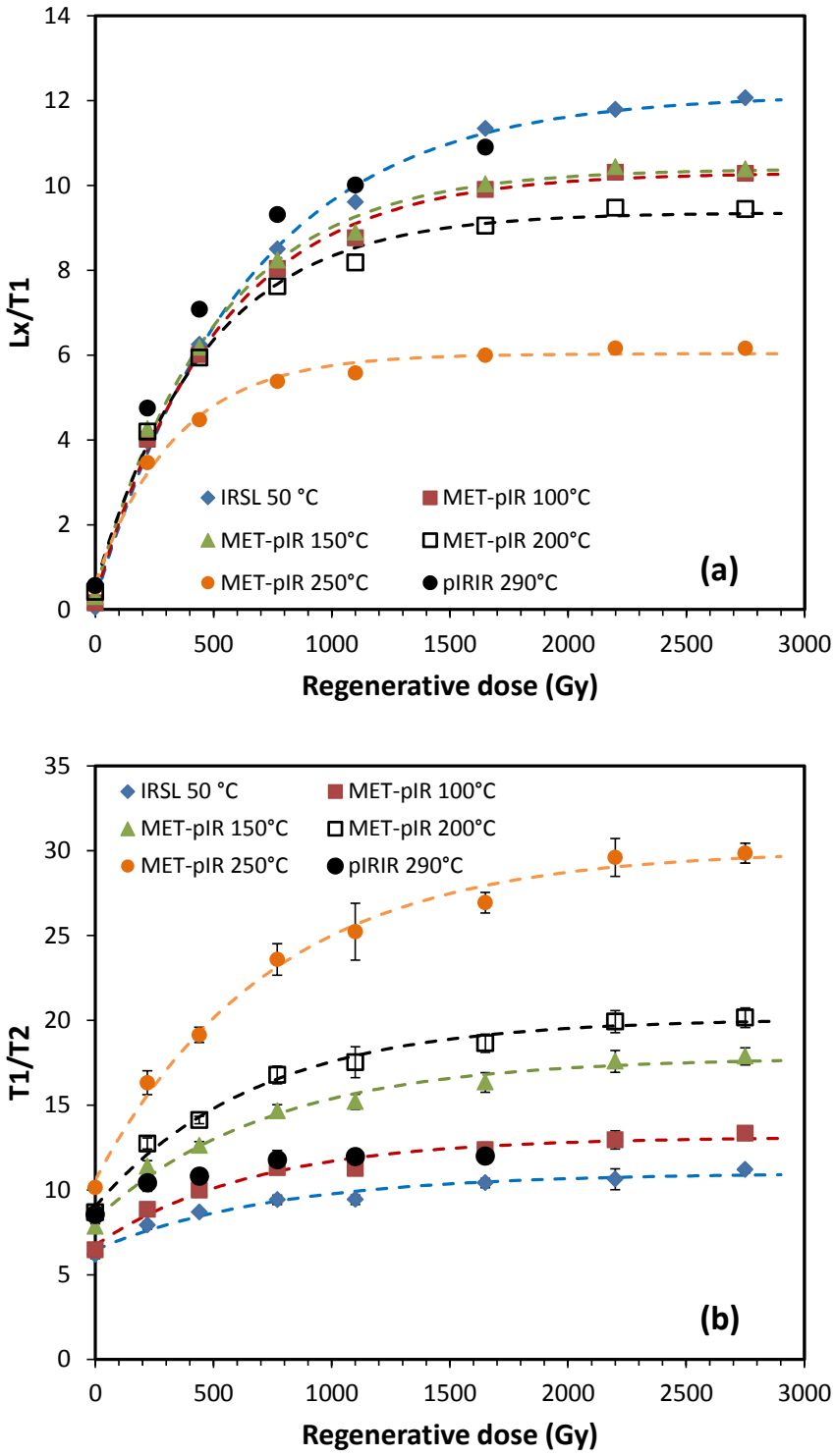
Lx/T1
Regenerative dose (Gy)
IRSL 50 °C
MET-pIR 100°C
MET-pIR 150°C
MET-pIR 200°C
MET-pIR 250°C
pIRIR 290°C
(a)
T1/T2
Regenerative dose (Gy)
IRSL 50 °C
MET-pIR 100°C
MET-pIR 150°C
MET-pIR 200°C
MET-pIR 250°C
pIRIR 290°C
(b)

Figure 8

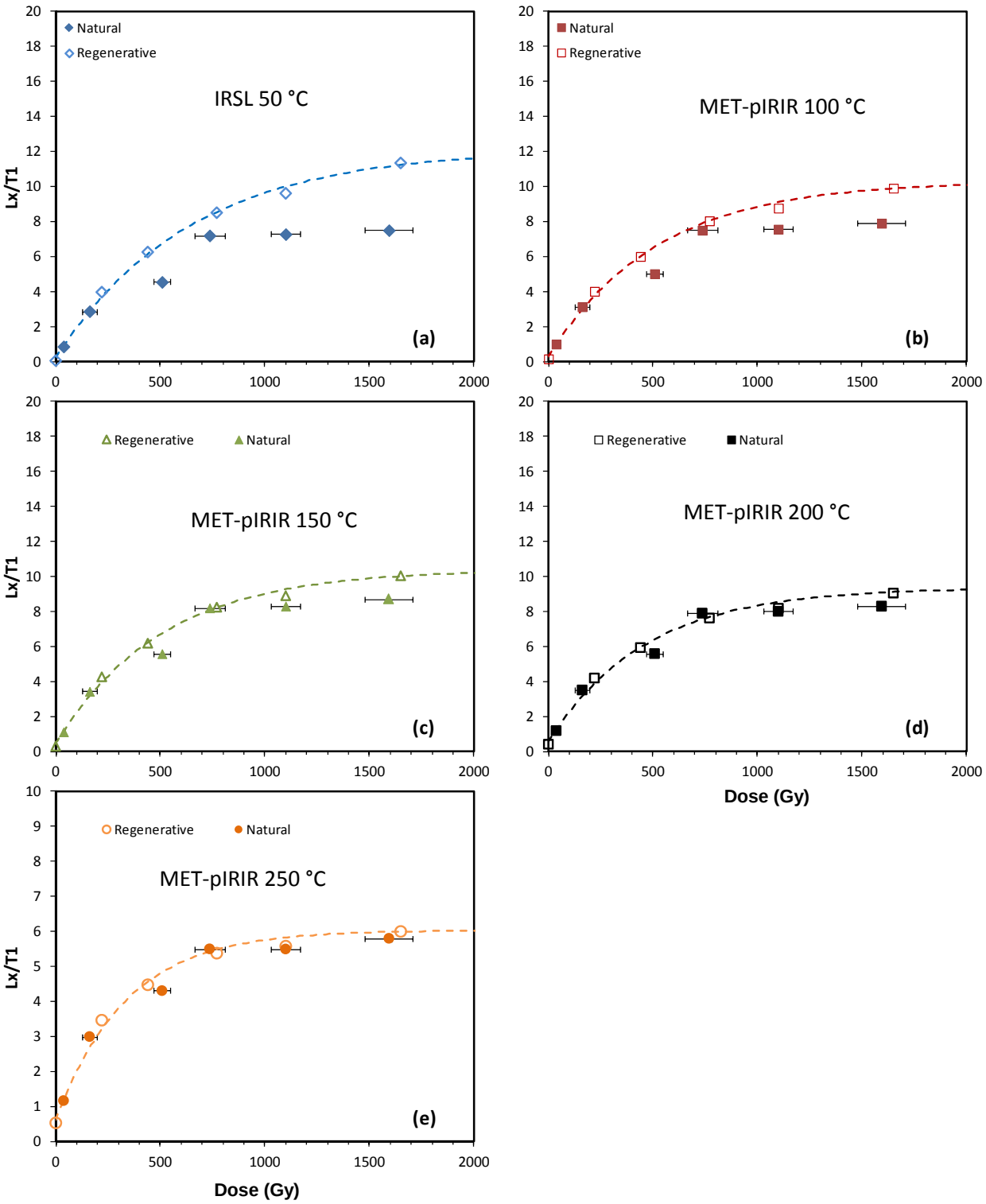
Natural
Regenerative
IRSL 50 °C
(a)
Natural
Regnerative
MET-pIRIR 100 °C
(b)
Regenerative
Natural
MET-pIRIR 150 °C
(c)
Regenerative
Natural
MET-pIRIR 200 °C
(d)
Regenerative
Natural
MET-pIRIR 250 °C
(e)
Lx/T1
Dose (Gy)

Figure 9

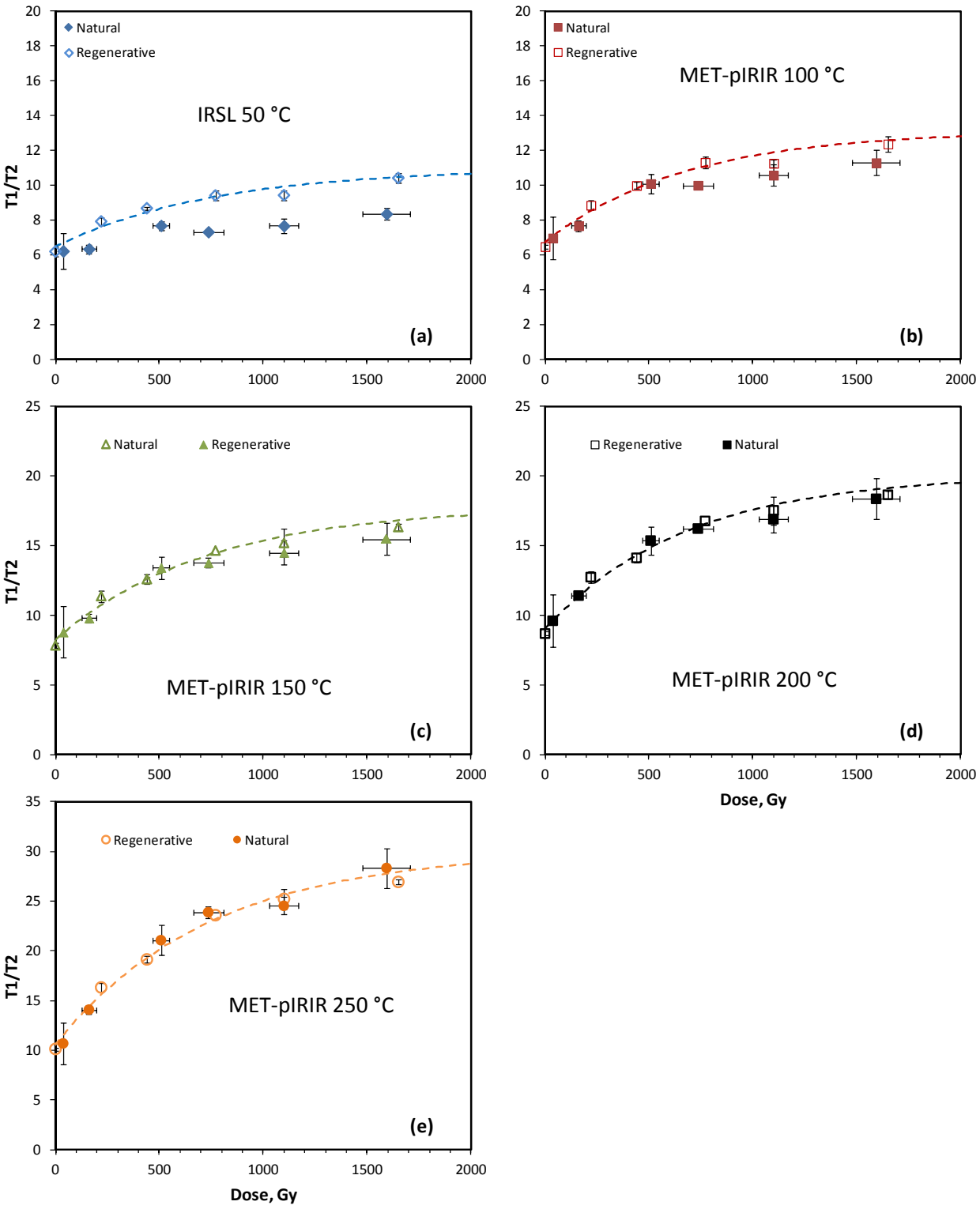
Natural
Regenerative
IRSL 50 °C
(a)
Natural
Regnerative
MET-pIRIR 100 °C
(b)
Natural
Regenerative
MET-pIRIR 150 °C
(c)
Regenerative
Natural
MET-pIRIR 200 °C
(d)
Regenerative
Natural
MET-pIRIR 250 °C
(e)
T1/T2
Dose, Gy

Figure 10

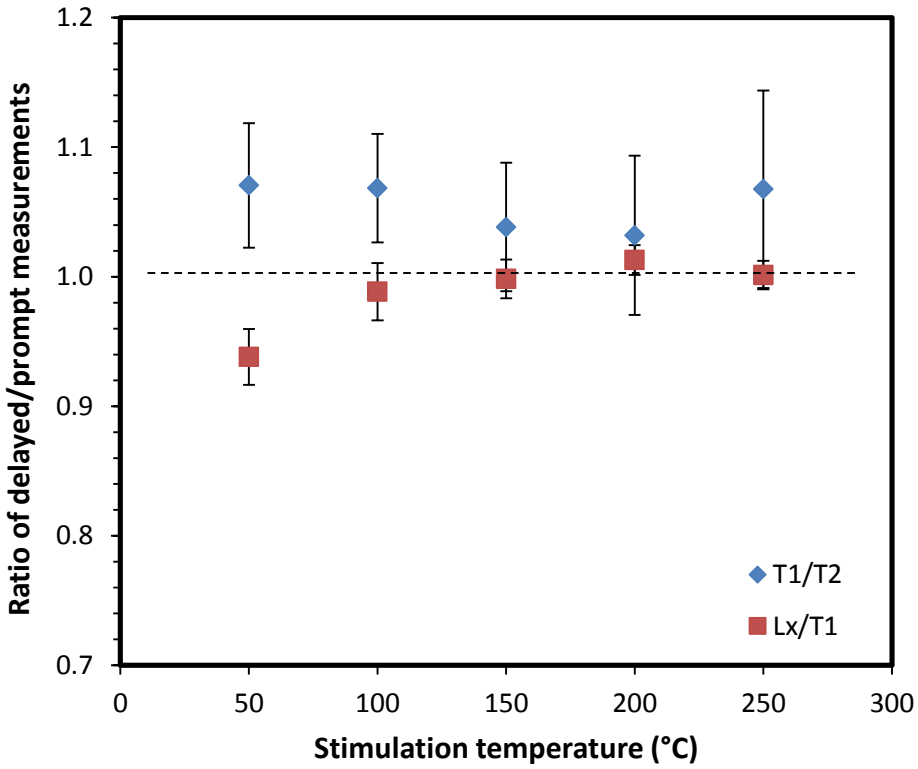
1.2
1.1
1.0
0.9
0.8
0.7
Ratio of delayed/prompt measurements
0
50
100
150
200
250
300
Stimulation temperature (°C)
T1/T2
Lx/T1

Figure 11

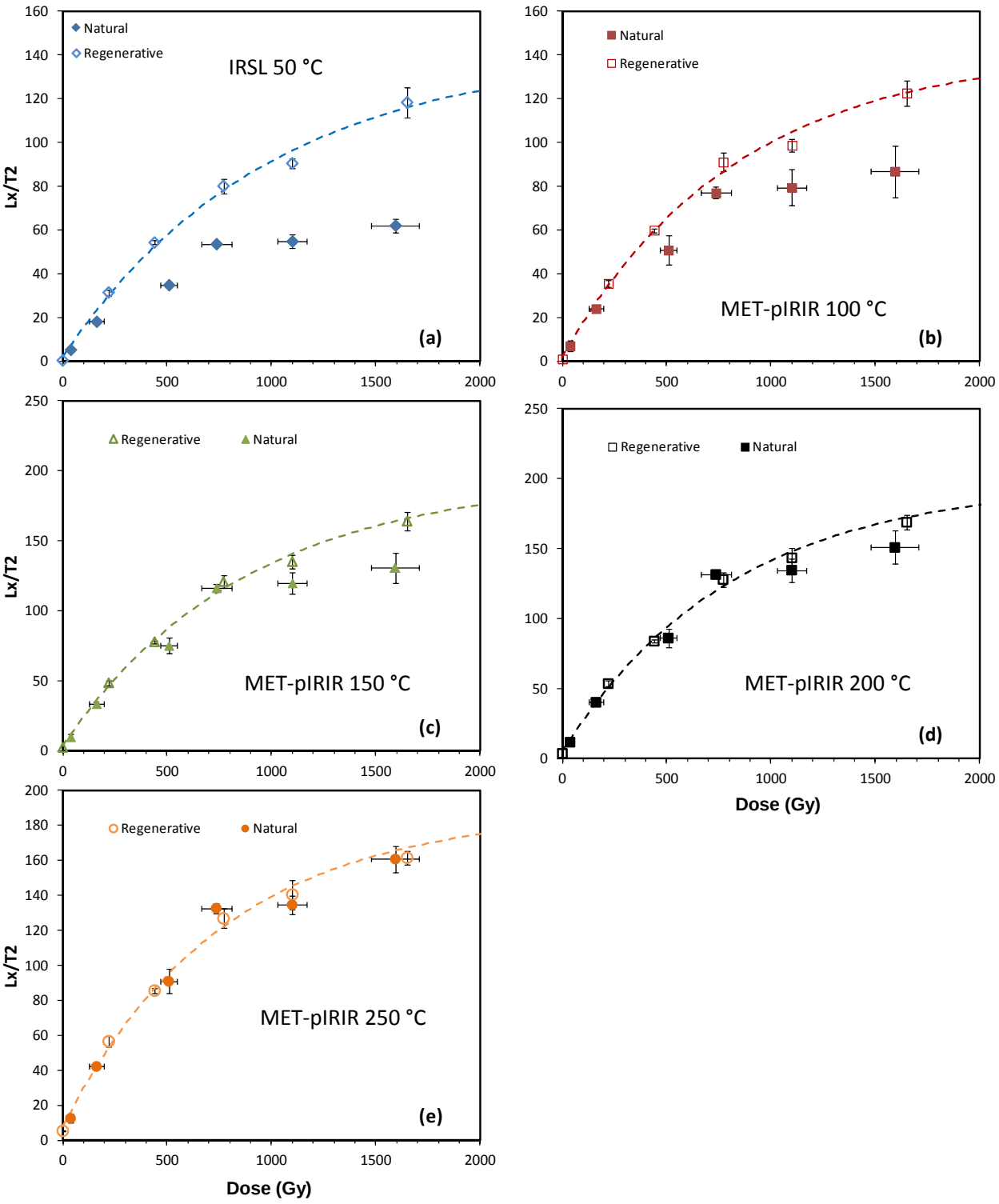
Natural
Regenerative
IRSL 50 °C
(a)
Lx/T2
Natural
Regenerative
MET-pIRIR 100 °C
(b)
Regenerative
Natural
MET-pIRIR 150 °C
(c)
Regenerative
Natural
MET-pIRIR 200 °C
(d)
Regenerative
Natural
MET-pIRIR 250 °C
(e)
Lx/T2
Dose (Gy)
Dose (Gy)

Figure 12

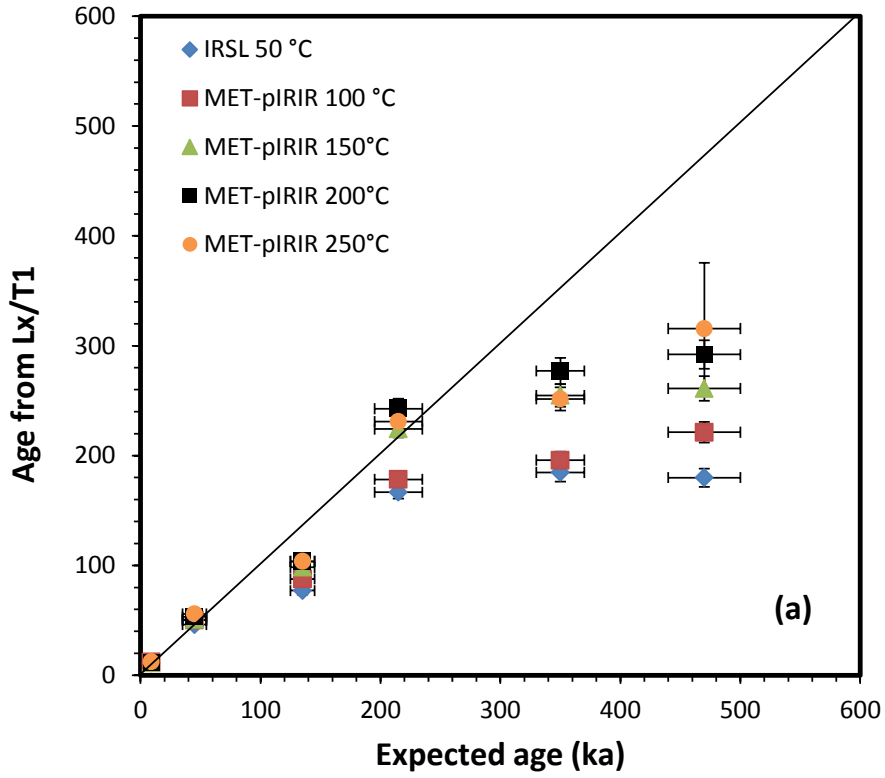
IRSL 50 °C
MET-pIRIR 100 °C
MET-pIRIR 150°C
MET-pIRIR 200°C
MET-pIRIR 250°C
Age from Lx/T1
Expected age (ka)
(a)
0
100
200
300
400
500
600

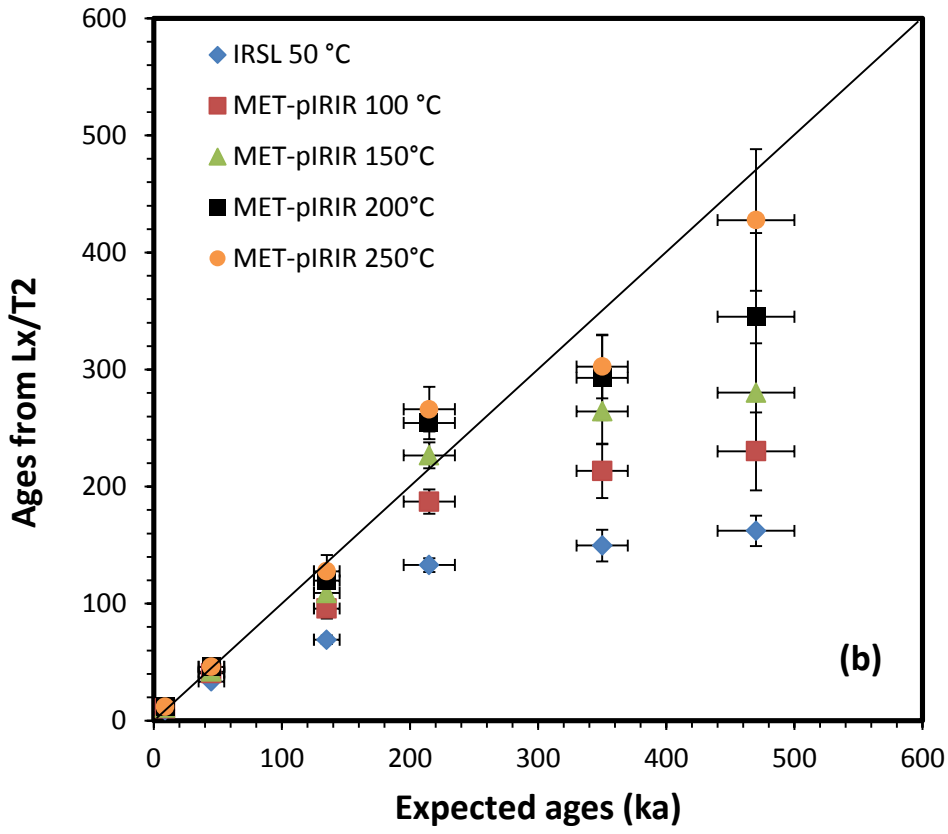
IRSL 50 °C
MET-pIRIR 100 °C
MET-pIRIR 150°C
MET-pIRIR 200°C
MET-pIRIR 250°C
Ages from Lx/T2
Expected ages (ka)
(b)
0
100
200
300
400
500
600

Figure 13

Table 1: Summary of the sampling depth, grain size, expected age, dose rate, expected D_e, and the equivalent dose (D_e) and age measured using the 250 ºC MET-pIRIR signals.

Sample	Depth (m)	Grain size (μm)	Expected age [a] (ka)	Dose rate [b] (Gy/ka)	Expected D_e [a] (Gy)	D_e (MET-pIRIR 250ºC) (Gy)			Age (MET-pIRIR 250ºC) (ka)		
						Lx/T1	Lx/T2	T1/T2	Lx/T1	Lx/T2	T1/T2
Sm1	2	180-212	9 ± 1	4.1 ± 0.2	37 ± 4	51 ± 2	49 ± 7	28 ± 82	12.5 ± 0.5	12.0 ± 1.7	7 ± 20
Sm3	8	125-150	45 ± 10	3.6 ± 0.2	161 ± 36	195 ± 12	165 ± 10	160 ± 20	56 ± 3	46 ± 3	45 ± 6
Sm5	19	180-212	135 ± 10	3.8 ± 0.2	508 ± 41	390 ± 15	480 ± 50	580 ± 120	104 ± 5	128 ± 14	154 ± 32
Sm6	26	90-125	215 ± 25	3.4 ± 0.1	735 ± 72	790 ± 20	910 ± 60	860 ± 80	231 ± 9	266 ± 19	252 ± 25
Sm6'	44	90-125	350 ± 20	3.1 ± 0.1	1099 ± 72	788 ± 22	950 ± 80	960 ± 98	252 ± 11	303 ± 27	306 ± 33
Sm8	65	150-180	470 ± 10	3.4 ± 0.1	1593 ± 114	1070 ± 190	1450 ± 230	1802 ± 592	316 ± 60	428 ± 61	531 ± 179

Note:

[a] The expected ages are based on stratigraphic comparisons among different sites in the Loess Plateau and on correlations of the grain size and magnetic susceptibility curves to the orbitally tuned Baoji section (Ding et al., 1994); see Sun et al. (1999) for the details of correlation. The expected ages, together with the dose rates, were used to estimate the expected D_e.

[b] The dose rates were obtained from measurements of current environmental radioactivity, together with the dose rate conversion factors of Adamiec and Aitken (1998). For calculation of the internal dose rate, the concentrations of K and Rb are assumed to be 13 ± 1% and 400 ± 100 μg/g (Huntley and Baril, 1997; Huntley and Hancock, 2001; Li et al., 2007; Zhao and Li, 2005), respectively.

Table 2: Multi-aliquot regenerative-dose (MAR) procedure used for multi-elevated-temperature post-IR IRSL (MET-pIRIR) measurements.

MET-pIRIR protocol		
Step	Treatment	Observed
1	Give regenerative dose, D_i [a]	
2	Preheat at 300°C for 60 s	
3	[b] IRSL measurement at 50°C for 100 s	$L_{x(50°C)}$
4	[b] IRSL measurement at 100°C for 100 s	$L_{x(100°C)}$
5	[b] IRSL measurement at 150°C for 100 s	$L_{x(150°C)}$
6	[b] IRSL measurement at 200°C for 100 s	$L_{x(200°C)}$
7	[b] IRSL measurement at 250°C for 100 s	$L_{x(250°C)}$
8	Give test dose, D_t	
9	Preheat at 300°C for 60 s	
10	[b] IRSL measurement at 50°C for 100 s	$T1_{(50°C)}$
11	[b] IRSL measurement at 100°C for 100 s	$T1_{(100°C)}$
12	[b] IRSL measurement at 150°C for 100 s	$T1_{(150°C)}$
13	[b] IRSL measurement at 200°C for 100 s	$T1_{(200°C)}$
14	[b] IRSL measurement at 250°C for 100 s	$T1_{(250°C)}$
15	Cut-heat to 600 °C	
16	Give test dose, D_t	
17	Preheat at 300°C for 60 s	
18	[b] IRSL measurement at 50°C for 100 s	$T2_{(50°C)}$
19	[b] IRSL measurement at 100°C for 100 s	$T2_{(100°C)}$
20	[b] IRSL measurement at 150°C for 100 s	$T2_{(150°C)}$
21	[b] IRSL measurement at 200°C for 100 s	$T2_{(200°C)}$
22	[b] IRSL measurement at 250°C for 100 s	$T2_{(250°C)}$

[a] For the 'natural' and sunlight-bleached samples, i= 0 and $D_0 = 0$. The entire sequence is repeated for several regenerative doses, including a zero dose and a repeat dose.

[b] For each IRSL measurement, an 'IR-off' period was applied to minimise the isothermal decay signal (Fu et al., 2012). That is, the aliquots were held for 10, 10, 20, 20 and 50 s at the stimulation temperatures of 50, 100, 150, 200, and 250 °C (steps 3-7, 10-14 and 18-22), respectively, before switching on the IR diodes to measure the IRSL signal.

Table 3. Summary of the characteristic saturation doses of the dose-response curves for various MET-pIRIR signals.

Signal	Characteristic saturation dose (D_0, in Gy) for the IRSL and MET-pIRIR signals at the specified stimulation temperature				
	50°C	100°C	150°C	200°C	250°C
Lx/T1	643 ± 37	518 ± 29	507 ± 32	466 ± 34	337 ± 30
T1/T2	766 ± 180	669 ± 119	730 ± 113	678 ± 84	741 ± 82
Lx/T2	987 ± 86	830 ± 67	875 ± 64	810 ± 57	766 ± 64